Hot Water-Treated Cow Waste Use as an Efficient Adsorbent for Cresol Red Dye and Chromium VI Removal from Aqueous Solutions

Ali El-Rayyes,[a,b] Ibrahim Arogundade,[c] Abimbola A. Ogundiran,[d,*] Mohamed Hefnawy,[e] Edwin Andrew Ofudje,[c] Ali El Gamal,[f] Lamia A. Albedair,[g] and Amnah Mohammed Alsuhaibani [h]

Hot water-treated cow waste (HWTCW) was used as an efficient, low-cost, and sustainable adsorbent for the removal of cresol red dye and chromium(VI) from aqueous solutions. Functional groups present on the biomass surface were identified by Fourier Transform Infrared Spectroscopy as -OH, C=O, C=C, and C-O. The scanning electron microscopy analysis showed the structure relating to plant tissue and rough surfaces that were heterogeneous and irregular, revealing the origin of the biomass to be cellulose, lignin, hemicellulose, and other water-soluble components. Maximum adsorption capacity was attained at biomass dosage of 40 and 50 mg, 120 and 140 min as the time of contact, pH of 4 and 3, and temperature of 40 and 45 °C for CR and Cr (VI) adsorption. The equilibrium data from the adsorption of CR and Cr (VI) followed Langmuir and Freundlich models with maximum uptake of 73.3 and 66.4 mg/g. For the adsorption of CR by HWTCW, a pseudo-first-order kinetic model provided a better fit, whereas a pseudo-second-order model provided a better fit for Cr (VI) ions adsorption. The analysis of Δ*H* gave positive values of 22.4 kJ/mol for CR and 46.0 kJ/mol for Cr (VI) indicating the endothermic process.

DOI: 10.15376/biores.20.2.3252-3285

Keywords: Adsorbent; Adsorption; Cow waste; Cresol red; Hexavalent chromium

Contact information: a: Center for Scientific Research and Entrepreneurship, Northern Border University, Arar, 73213, Saudi Arabia; b: Chemistry Department, College of Science, Northern Border University, Arar, Saudi Arabia; c: *Department of Chemical Sciences, Tai Solarin University of Education, Ijagun, Ijebu-Ode, Ogun State, Nigeria; d: Department of Chemical Sciences, Mountain Top University, Ogun State, Nigeria; e: Department of Pharmaceutical Chemistry, College of Pharmacy, King Saud University, Riyadh 11451, Saudi Arabia; f: Department of Pharmacognosy, College of Pharmacy, King Saud University, Riyadh 11451, Saudi Arabia; g: Department of Chemistry, College of Science, Princess Nourah bint Abdulrahman University, P.O. Box 84428, Riyadh 11671, Saudi Arabia; h: Department of Sports Health, College of Sport Sciences & Physical Activity, Princess Nourah bint Abdulrahman University, P.O. Box 84428, Riyadh 11671, Saudi Arabia; *Corresponding author: abimbolaogundiran701@gmail.com*

INTRODUCTION

Water pollution from organic contaminants including industrial effluent, dyes, oil spillage, pesticides, and herbicides is a significant concern as it degrades the quality of water and poses high risks to the environment and public health (Uzosike *et al*. 2022; Ofudje *et al*. 2023). Many industries, including plastics, pharmaceuticals, printing, textile, cosmetics, rubber, paper, leather, food processing, agriculture, and hair coloring, use dyes extensively and often discharge them as by-products into water bodies (Tkaczyk *et al*. 2020; Ogundiran *et al*. 2022). Dyes can form carcinogenic compounds in the body

if inhaled or ingested *via* food and, in severe cases, block sunlight and oxygen from penetrating water bodies (Konicki *et al*. 2017; Ofudje *et al*. 2022). When industrial waste and effluents released into municipal areas are not controlled, it is a major factor contributing to deteriorating water quality (Uzosike *et al*. 2022; Ofudje *et al*. 2023). Even small amounts of dye-laden wastewater can affect the appearance of receiving streams, while the carcinogenic and mutagenic properties of dyes can disrupt aquatic life and food webs (Ofudje *et al*. 2020; Delpiano *et al*. 2021).

Cresol red dye, for instance, is a widely used phenolic organic compound in antiseptics and disinfectants that can cause physiological reactions, such as vomiting, insomnia, and cramps, if accidentally touched (Herbache *et al*. 2015; Zhang *et al*. 2023). Ingesting cresol, however, poses far greater risks, including damage to the nervous system and internal organs, and can even be fatal (Guo *et al*. 2021; Yang *et al*. 2022). Once introduced into the environment through wastewater discharge, this harmful organic compound can have long-lasting negative effects on water ecosystems, potentially causing irreversible damage (Guo *et al*. 2021; Yang *et al*. 2022). In a literature report by the United States Environmental Protection Agency (US EPA), the upper limit of any phenolic compounds should not surpass 12 μg/L (Taleb *et al*. 2021).

Meanwhile, chromium (VI) occurs naturally and is widely used in various industries including mining, leather tanning, paint pigments, refractories, wood preservation, textile, aerospace, and electroplating (Misbah *et al*. 2016; Islam *et al*. 2019). Industrial leakage, improper disposal practices, and poor storage are some of the ways through which significant amounts of chromium are discharged into the environment. Natural sources, such as chromium ores, which includes chromite deposits in bedrock and soil, also contribute to increased chromium levels in the environment (Zhang *et al*. 2018). The extreme toxic nature of hexavalent chromium means that it could become carcinogenic, mutagenic, and teratogenic to living organisms, with greater water solubility and mobility, which makes it more toxic when compared with Cr(III) (approximately 300 times more toxic) (Shi *et al*. 2020). As a result, it is crucial to search for new materials that can effectively neutralize such pollutants, transforming them into harmless and non-toxic substances.

Contaminants removal from wastewater can be achieved *via* methods such as coagulation, photocatalysis, ion exchange, membrane processes, advanced oxidation processes, flocculation, and adsorption (Taleb *et al*. 2021; Uzosike *et al*. 2022; Ofudje *et al*. 2023). The selection of cresol red dye and chromium(VI) [Cr(VI)] for this study is driven by their prevalence in industrial effluents and the significant challenges associated with their removal from aqueous solutions. The challenges in removal of chromium (VI) has to do with the fact that these traditional removal methods often face challenges such as high operational costs, generation of secondary waste, and the need for skilled manpower. Additionally, the efficiency of these methods can be compromised by the presence of other contaminants and varying water chemistry (Abayneh *et al*. 2022). Cresol red dye removal on the other hand is challenging due to their synthetic origin and complex molecular structures, which confer stability and resistance to biodegradation and as such, conventional treatment methods may be ineffective, leading to the persistence of these dyes in the environment and potential ecological impacts (Badr Khudhair *et al*. 2015). Given the environmental persistence and health hazards associated with Cr(VI) and cresol red dye, there is a pressing need to develop efficient, cost-effective, and sustainable removal methods. Exploring alternative adsorbents, such as hot water-treated

cow waste, offers a promising avenue to address these challenges, providing potential benefits in terms of availability, low cost, and environmental sustainability.

Of these traditional approaches, adsorption is one of the most effective, cost efficient, and simple techniques for producing good quality water that is often utilized (Kanawade *et al*. 2011). The adsorbent that is widely deployed in this adsorption process is known as 'activated carbon', which is expensive due to its high level of purity, often leading to its setback in the treatment of wastewater. Various researchers have explored cheap adsorbents, including agricultural waste (Lai, 2021), apatite derived from bone meal (Ofudje *et al*. 2020), bagasse (Kumar *et al.* 2020), snail shells (Ogundiran *et al*. 2022), vlignin-based composite (Shi *et al*. 2020), sugarcane waste (Ofudje *et al*. 2014), seed coat of *Heinsia crinita* (Dawodu *et al*. 2020), Algerian sodium (Na)-clay (Herbache *et al*. 2015), *Artocarpus nobilis* fruit peel (Samaraweera *et al*. 2020), Teff husk (Adane *et al.* 2020), and chickpea (Ozsin *et al*. 2019) in eliminating dyes and other contaminants from the environment. The strong affinity for pollutants towards these low-cost adsorbents is ascribed to the availability of cellulose and other functional properties available on the adsorbent surface.

Kuncoro *et al*. (2017) developed an adsorbent from a mixture of algae waste and bentonite, characterized by FTIR and SEM-EDX analyses, which indicated successful Pb^{2+} adsorption through observed shifts in wave numbers and the presence of lead on the adsorbent surface. The findings suggest that this adsorbent is a promising method for treating lead-contaminated wastewater. Neolaka *et al*. (2024) successfully developed a green adsorbent from banana peel activated with lime juice, characterized by structural changes such as a bonded O–H group at 3300 cm^{-1}, C–H stretching at 2921 cm^{-1}, and increased porosity, achieving a Rhodamine B adsorption capacity of 70 mg/L in 10 minutes at pH 6 and 323 K. Thermodynamic analysis showed an exothermic and spontaneous process (ΔH = −25.3 kJ/mol, ΔS = 0.572 kJ/mol), highlighting its potential for wastewater treatment. The evaluation of horn snail (*Telescopium* sp) and mud crab (*Scylla* sp) shell powders as low-cost adsorbents for removing Cu^{2+} from synthetic wastewater was done by Darmokoesoemo *et al*. (2016). Optimal adsorption occurred at 2 hours, achieving capacities of 4.59 mg/g for horn snail and 4.32 mg/g for mud crab shells. The FT-IR analysis identified functional groups such as C=O and O-H in both adsorbents, with mud crab shells also exhibiting N-H bending, while SEM-EDX analysis of horn snail shells revealed ion exchange between Ca^{2+} and Cu^{2+}, confirming their potential for heavy metal removal in wastewater treatment. Raseed *et al*. (2020) evaluated the adsorption behavior of Cu^{2+}, Ni^{2+}, and Zn^{2+} ions using *Archontophoenix alexandrae* in single (SMS), bi-metal (BMS), and tri-metal systems (TMS). The results indicated that Cu^{2+} exhibited the highest adsorption capacity, with its presence suppressing the adsorption of Ni^{2+} and Zn^{2+}. They concluded that *A. alexandrae* is an effective biosorbent for removing toxic metals from industrial effluents.

Existing adsorbents for removing contaminants such as cresol Red dye and chromium(VI) from aqueous solutions often face significant challenges related to cost, efficiency, and environmental impact, while traditional materials, such as activated carbon for instance are expensive to produce and regenerate, limiting their widespread application in large-scale wastewater treatment (Sanad *et al*. 2024). Additionally, many conventional adsorbents exhibit limited adsorption capacities, necessitating large quantities to achieve effective contaminant removal, which further escalates operational costs and complexity (Satyam and Sanjukta 2024). Moreover, the production and disposal of some synthetic adsorbents can introduce secondary environmental concerns,

including the generation of hazardous by-products and non-biodegradable waste (Jana *et al*. 2024). These limitations underscore the need for developing innovative, cost-effective, and environmentally friendly adsorbents, such as hot water-treated cow waste, to enhance the sustainability and efficiency of wastewater treatment processes.

Cow waste, a renewable resource material, primarily consists of the undigested cellulose-based feed excreted by livestock such as bulls and cows. Composed mainly of lignin, cellulose, and hemicelluloses, cow waste is composed of feces and urine in a 3:1 ratio (Gupta *et al.* 2016; Anuar *et al.* 2019). If not properly managed, these animal by-products can cause environmental issues such as air pollution in forms of greenhouse gases, including methane, offensive odors, public health hazards from water contamination, and infectious pathogens (Gupta *et al.* 2016; Anuar *et al.* 2019).

The sorption ability of these cellulose materials can be harnessed, and cow waste is a potential green material that might be utilized as cheap pollutant removal in diverse applications. Garba *et al*. (2019) studied cow dung as affordable and efficient adsorbent for glyphosate (GLY) and its metabolite, aminomethylphoshonic acid (AMPA). It was found that the cow dung contained amines, phenol, ethers, and carboxylic functional groups, and it had high affinities for GLY and AMPA respectively. It also demonstrated strong adsorption capacities and minimal desorption. The ability of dry cow dung powder to remove toxic heavy metal ions, including Cr(III), Cr(VI), and Cd(II), was successfully demonstrated by Barot *et al.* (2012). Batch equilibration experiments showed that the cow dung powder is an eco-friendly and efficient biosorbent for heavy metal removal from aqueous solutions, offering a promising solution for wastewater treatment. Cow dung ash was investigated by Ayyappan and Elangovan (2017) as a low-cost adsorbent for chromium (Cr) removal from industrial wastewater, a critical environmental concern due to Cr's toxicity. The study found optimal chromium removal with 6 g/L of cow dung ash in 1000 mL solution within 3 hours, while pH showed minimal impact on the adsorption process. Elaigwu *et al*. (2009) reported that the adsorption efficiency of Pb(II) ions onto activated carbon derived from cow dung is influenced by pH levels and that the highest removal efficiency was observed at pH 2.0, which decreased at pH 3.0, followed by a steady increase between pH 4.0 and 8.0. Qian *et al*. (2008) investigated the adsorption of methylene blue (MB) onto activated carbons (ACs) derived from cattle manure compost (CMC) through $ZnCl_2$ activation. The adsorbents demonstrated exceptional performance in MB adsorption, which can be attributed to their high surface area, substantial mesopore volume, and elevated nitrogen content. Using cow waste as an adsorbent not only capitalizes on its low economic value but also helps mitigate its harmful impact on the environment.

The primary objective of this research was to evaluate the effectiveness of hot water-treated cow waste (HWTCW) as an efficient, low-cost, and sustainable adsorbent for the removal of cresol red dye and chromium(VI) from aqueous solutions. Determination of the optimal conditions (*e.g*., pH, contact time, adsorbent dosage, and initial contaminant concentration) for the adsorption of cresol red dye and chromium(VI) onto HWTCW was carried out. The study also examined the interaction mechanisms between HWTCW and the contaminants to elucidate the adsorption process. Finally, the potential for regenerating and reusing HWTCW in multiple adsorption-desorption cycles to determine its practical applicability was performed.

EXPERIMENTAL

Materials

Preparation of adsorbate solution

Chromium (VI) ions and cresol red aqueous solution were made using chemicals purchased from Sigma Aldrich, India and deployed without any purification because they were of analytical grade. Adsorbate stock solutions were prepared by dissolving 3.824 g of CR and 2.75 g of Cr (VI) in 1000 mL of distilled water inside a volumetric flask and made to the mark. Several other solutions were made from the stock solution through dilution principle for the analysis.

Cow waste adsorbent preparation

The cow waste was obtained from Owode Eleran, Imowo, Ijebu-Ode, Ogun State of Nigeria. It was collected at the point of discharge from the cow on the field. The samples were treated with hot water for 10 min at a temperature of 100 °C, washed with distilled water several times and filtered. Then, residue cow waste was sun dried for 7 days to remove its odour and kill any active maggots that may be present. The hot water-treated cow waste was later oven dried to dry off other moisture present, ground into powder using mortar and pestle, and referred to as hot water-treated cow waste (HWTCW).

Methods

Cow waste structural analysis

The structural characterization of the adsorbent was performed using multiple techniques. Surface morphology was analyzed through Scanning Electron Microscopy (SEM-EDX; EVO MA-10, Carl Zeiss, Jena, Germany). Fourier Transform Infrared (FT-IR) spectroscopy was employed to identify surface functional groups using the attenuated total reflectance (ATR) method, with spectra recorded in the range of 4000 to 400 cm^{-1} at a resolution of 4 cm^{-1} (Bruker Tensor 27 spectrophotometer; Bruker Corporation, Billerica, MA, USA). X-ray diffraction (XRD) measurement was conducted using an X'PERT Pro PANalytical diffractometer (Malvern Panalytical, Almelo, Netherlands) with Cu Kα radiation, with diffraction peaks recorded at 2θ angles between 15° and 30° and a step size of 0.013. The biomass zeta potential was measured with a Zetasizer Nano ZS (Malvern, UK). Prior to measurement, 10 mg of the sample was finely ground and dispersed in distilled water to enhance light scattering. Next, the sample was sonicated for 10 min to break up particle agglomerates and ensure uniform distribution.

Adsorption study

A 25-mL aliquot of the pollutant was transferred into a beaker, followed by pH adjustment using a dilute solution of either 0.1 M HNO_3 or NaOH in the pH range of 2 to 8. Next, 40 mg of HWTCW was added to the beaker containing the pollutant solutions, and an orbital shaker was used to agitate the mixture at 100 rotation per minute (rpm). At specific time intervals, aliquots of the pollutant solution were collected for analysis using a UV-visible spectrophotometer (model V-570; ASCO Corporation, Tokyo, Japan) after filtration. For the Cr(VI) analysis, prior to the UV-visible spectrophotometer analysis, the residual chromium ion concentration was measured using the diphenylcarbazide method at 570 nm. Since the detection of Cr(VI) was based on a redox-type test, the presence of Cr(III) was not detected. The adsorption experiment was repeated thrice, and the average

values reported. The adsorbed amount of the pollutant (Q_e) in mg/g and the percentage removal (%R) were analysed as follows,

$$Q_e = \frac{C_o - C_e}{m} \times v \quad (1)$$

$$\%R = \frac{C_o - C_e}{C_o} \times 100 \quad (2)$$

where C_o and C_e represent the initial and supernatant concentrations of the pollutant in mg/L, respectively. The volume of the pollutant solution is denoted as V in L, and the mass of HWTCW used is indicated as m in g.

RESULTS AND DISCUSSION

Cow Waste Characterizations

The FT-IR spectra of cow waste with and without pollutant load adsorbent are presented in Fig. 1. In the FT-IR study of the cow waste without pollutant load, the peak seen at 3463 cm^{-1} is typically associated with O-H stretching, which suggests hydroxyl groups and water of cellulose and lignin (Jaramillo-Quiceno *et al*. 2018; Yang *et al*. 2023), whereas the peak at 3025 cm^{-1} corresponds to C-H of alkenes. The peak that usually indicates the of C-H stretching in aliphatic compounds, common in organic matter such as cellulose and hemicellulose components, was observed at 2915 cm^{-1} (Ilyas *et al*. 2018; Yang *et al*. 2023). The peak seen at 1735 cm^{-1} is ascribed to C=O stretching. This was likely from unconjugated ketones and could also be associated with hemicellulose (Jaramillo-Quiceno *et al*. 2018; Yang *et al*. 2023), while the one seen at 1674 cm^{-1} may also suggest the presence of C=O stretching, particularly from amides or conjugated systems. The observed peaks at 1505 cm^{-1} and 1458 cm^{-1} are associated with C-C bending or C-H bending vibrations, possibly indicating aromatic compounds or CH_2 groups. The typical peak that is associated with C-O stretching, indicative of alcohols, ethers, or carbohydrates, is seen at 1098 cm^{-1}, whereas the lower wavenumber peaks that may suggest the presence of substituted aromatic compounds were found around 764 cm^{-1} and 650 cm^{-1}.

The FT-IR spectrum of cow waste after adsorption indicated various changes to the vibrational modes of the functional groups present. For instance, a new peak was seen at 3425 cm^{-1}, which is associated with O-H stretching vibrations from cellulose and lignin. Meanwhile, new peaks corresponding to C-H vibrations from organic matter in cellulose and hemicellulose were noticeable at 3016 and 2920 cm^{-1}. Similarly, a new sharp peak that may be attributed to carbonyl (C=O) stretching vibrations possibly from aldehydes, ketones, or esters was observed at 1730 cm^{-1}, whereas a new band that could be due to C=C vibrations was seen at around 1686 cm^{-1}. Furthermore, the peak corresponding to C-O stretching was noticed at 1026 cm^{-1}, while the new peaks seen at 825 cm^{-1}, 730 cm^{-1}, and 685 cm^{-1} could represent bending vibrations associated with C-H in-plane or out-of-plane deformations. Overall, the spectrum indicates that cow waste contains a complex mixture of organic compounds that may have interacted with adsorbates, causing changes in the functional composition of the biomass. This suggests that functional groups such as -OH, C=O, C=C and C-O could have been involved in the adsorption of cresol red and chromium (VI) ions.

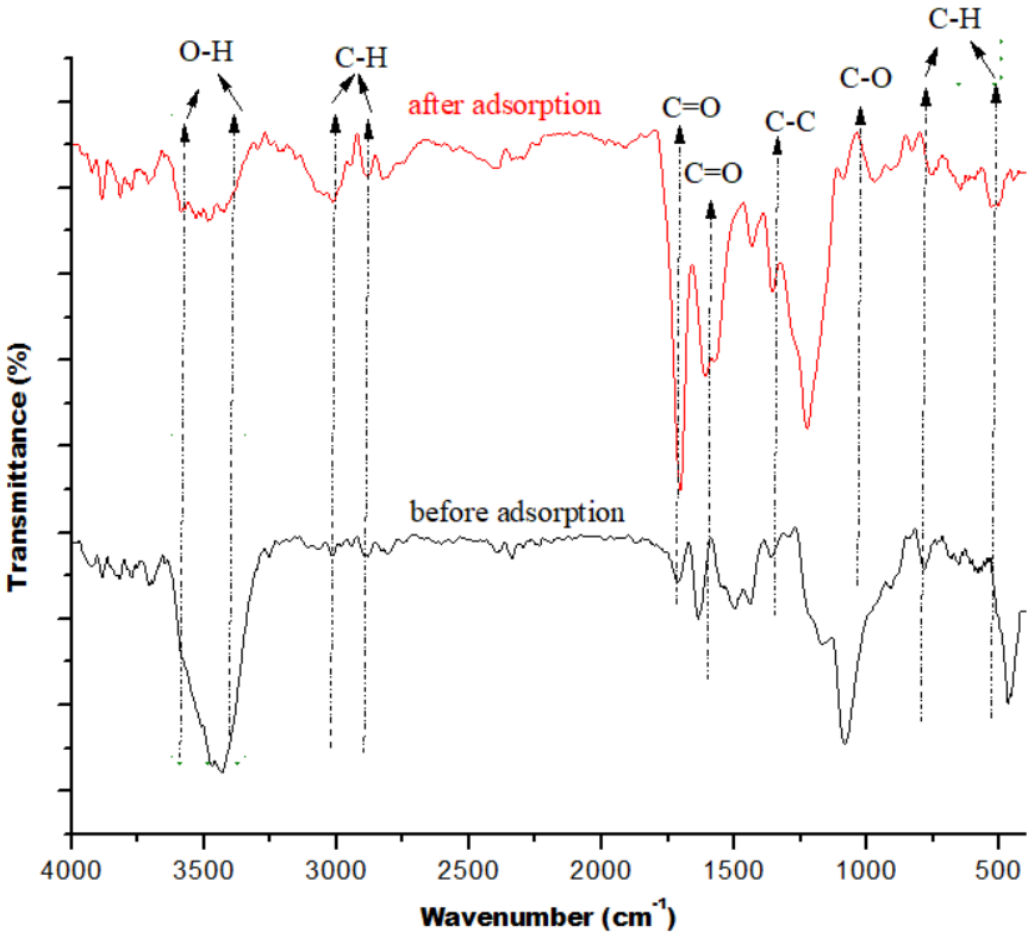

Fig. 1. FT-IR spectra of cow waste earlier and after adsorption process

X-ray diffraction (XRD) evaluation of hot water-treated cow waste prior to and after adsorption process, which is aimed at identifying the mineral composition present in the biomass, is shown in Fig. 2. Specific peaks at 2θ values around 15.04° and 22.65° were due to the (110), and (200) planes of cellulose I (Reddy *et al.* 2018; Wahlstrom *et al.* 2022) were seen in the XRD of the hot water-treated cow waste before adsorption. While the peak at around 15.04° may correspond to organic structures, the peak observed at around 22.65° could indicate crystalline materials, such as calcite or other minerals, found in cow waste. The XRD analysis of cow waste after adsorption experiments indicates changes in the crystalline structure due to the interaction with adsorbates. The observed peak at 22.65° in the biomass prior to experiments completely disappeared, while the peaks observed at 15.04° changed to 15.01°. Similarly, the interactions between the adsorbent and adsorbate may result in chemical reactions that alter the material's phase composition, and such transformations can lead to the emergence of new phases and the disappearance of characteristic peaks associated with the original material. Furthermore, changes in the sample's preferred orientation during the adsorption process can affect the intensity and presence of diffraction peaks pattern.

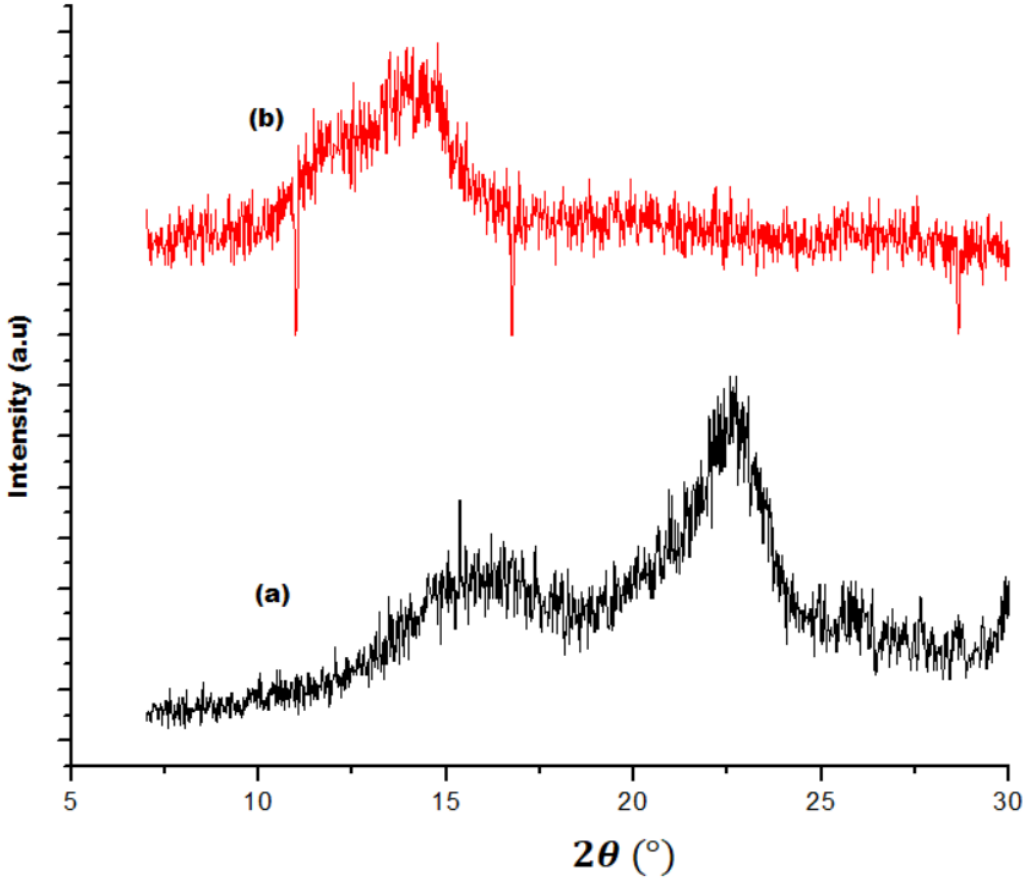

Fig. 2. XRD spectra of cow waste (a) before and (b) after adsorption process

The SEM analysis of the cow waste fibers with and without adsorbate load is as illustrated in Fig. 3. In the image corresponding to hot water-treated cow waste without adsorbate load (Fig. 3a), structure relating to plant tissue and rough surfaces that were heterogeneous and irregular were observed in the samples, which revealed the origin of the biomass to be cellulose, lignin, hemicellulose, and other water-soluble components. As for the sample corresponding to hot water-treated cow waste loaded with pollutant (Fig. 3b), though the surface still possesses characteristics of a cellulose or lignin, the surface appeared to be smoother with appearance of surface coverage suggesting the possible adherence of the molecules of the adsorbate onto the surface of the biomass. Specifically, the plant-based structure visible before adsorption became less prominent, which might have been covered by the adsorbed pollutants and this clear distinction between the SEM of cow waste with and without adsorbate could be due to surface coverage by pollutants.

The elemental composition of the hot water-treated cow waste revealed the following compositions O (62.0%), C(26.54%), Si (7.78%), and Ti (3.08%), as depicted in Fig. 3c. The high oxygen content indicates the presence of oxygenated compounds, such as organic material and oxides. Cow feces are known to contain considerable amounts of organic matter such as cellulose, hemicellulose, and lignin, all of which are rich in oxygen. The high oxygen percentage also suggests the presence of water (moisture) or hydrated compounds, which is common in biomass materials. The oxygen could also be present due to metal oxides formed on the surface (*e.g.*, silicon dioxide),

which might be involved in adsorption or surface modification. Carbon is typically abundant in cow feces due to its organic nature, which includes plant material, microbial biomass, and other organic residues, while silicon is often found in the form of silica (SiO_2), which is naturally present in soil and may be found in cow feces due to the animal's diet or environmental exposure. Silica is a known adsorbent material and can contribute to the overall adsorption capacity of the cow feces. Its presence in cow feces can improve the mechanical stability of the material and help with the adsorption of organic and inorganic contaminants. The presence of titanium dioxide suggests that the cow waste may have been contaminated through food or where it was deposited.

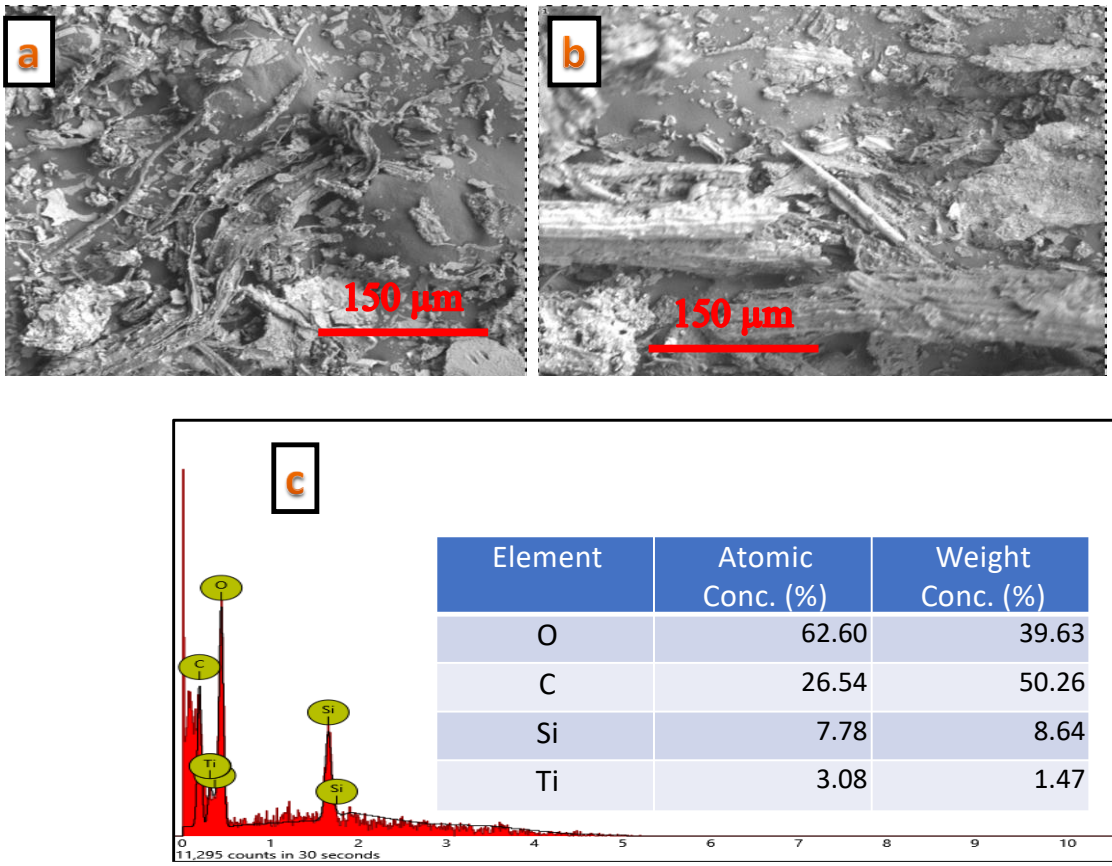

Element	Atomic Conc. (%)	Weight Conc. (%)
O	62.60	39.63
C	26.54	50.26
Si	7.78	8.64
Ti	3.08	1.47

Fig. 3. SEM of HWTCW (a) before, (b) after adsorption, and (c) EDS analysis of cow waste

Adsorbent Dosage Study

The availability and accessibility of adsorption sites are influenced by the biomass dosage, which was varied in this study from 10 g to 70 mg. Figure 4 presents the effect of biomass dosage on removal efficiency. It was noticed that the percentage removal of CR and Cr (VI) increased as the amount of HWTCW increased, with maximum removal rates of 85.6% for CR at 40 mg and 77.2% for Cr (VI) at 50 mg of HWTCW dosage. This surge in removal potency can be ascribed to the higher adsorbent concentration, which provided more surface area and active sites on the cow waste, allowing more pollutants to be adsorbed. Higher dosages can lead to particle aggregation, reducing the available surface area and active sites for adsorption (Alghamdi *et al*. 2019). Also, excess adsorbent may result in many active sites remaining unsaturated, leading to a lower adsorption per unit mass (Ali *et al*. 2023). More also, increasing adsorbent dosage can

decrease the concentration gradient between the solute in solution and on the adsorbent surface, diminishing the driving force for adsorption.

Ameer and Mutah (2015) also reported that increasing the adsorbent weight enhanced CR uptake using tire rubber recycled waste, with removal rates rising from 72% to 79%. Similarly, Herbache *et al*. (2015) found that the adsorption of o-cresol by Algerian Na-clay improved with higher adsorbent doses, reaching a maximum adsorption of 99.6% at 15 mg/250 mL. El Kassimi *et al.* (2023) observed a similar trend in the adsorption of Cr (VI) using medlar and *Cucumis melo* activated carbons, attributing the increased adsorption to the greater surface area and number of active sites available with higher adsorbent mass.

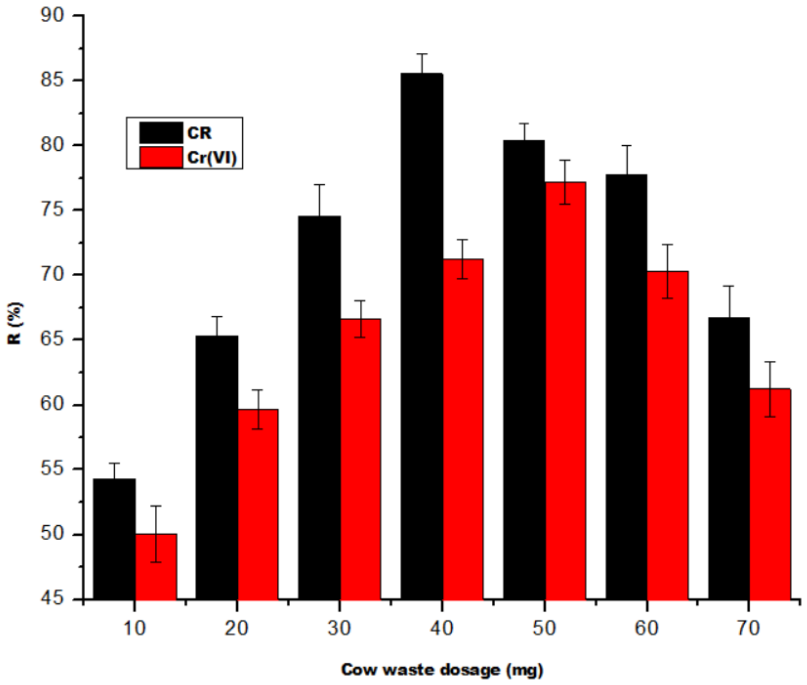

Fig. 4. Role of HWTCW dosages on the adsorption of CR and Cr (VI)

Studies on varied contaminants' concentration and contact time on the uptake of CR an Cr (VI)

The behavior of adsorption capacity on its response to variation of contact time and initial pollutant concentration as it affects the uptake of the pollutants were evaluated using varying agitation times and initial concentrations of cresol red dye and hexavalent chromium, as shown in Figs. 5 and 6. The adsorption capacity increased with the contact time, eventually reaching equilibrium at 120 min for cresol red dye and 140 min for hexavalent chromium. The amount removed in the case of cresol red at 300 mg/L of contaminant rose from 24.3 to 77.9 mg/g when the contact time was increased from 20 to 120 min (Fig. 5), whereas for the hexavalent chromium, the amount removed surged from 21.2 to 69.7 mg/g at the same contaminant concentration but at an increased contact time from 20 to 140 min (Fig. 6). The rapid initial increase in adsorption is likely due to more vacant active sites on the surface of HWTCW. However, the slower rate of adsorption in the later stages is attributed to the gradual diffusion of pollutant molecules into the adsorbent's pores, as the external sites become fully occupied. In a report by Ameer and Mutah (2015), the rate of adsorption of cresol red dye was said to have been enhanced

when the duration of contact with recycled waste tire rubber adsorbent increased from 7 to 21 days and that the best removal efficiency of 82% was reached in 21 days. Herbache *et al.* (2015) noted that the adsorption capacity of kaolin and montmorillonite for o-cresol adsorption was about 8.4 and 7.98 mg/g, respectively, and that a rapid initial step was observed until the process reached equilibrium at 250 min. Misbah *et al*. (2016) reported a linear increase in adsorption capacity with contact time and that 30 min was enough to attain equilibrium. They opined that the Cr(VI) rate of uptake at the initial stage was fast, and it thereafter declined progressively until equilibrium was attained. They concluded that the lower rate of adsorption towards the last stage of the reaction could be due to the difficulty experienced by the adsorbate molecules to fill up the leftover active vacant sites due to forces between the bulk phase and molecules of the solid. In a literature report by El Kassimi *et al*. (2023), during the uptake of Cr (VI) by *medlar* activated carbon and *Cucumis melo* activated carbon a rapid early removal of Cr (VI) was seen and was ascribed to more sites of adsorption available on the surface of the biomass.

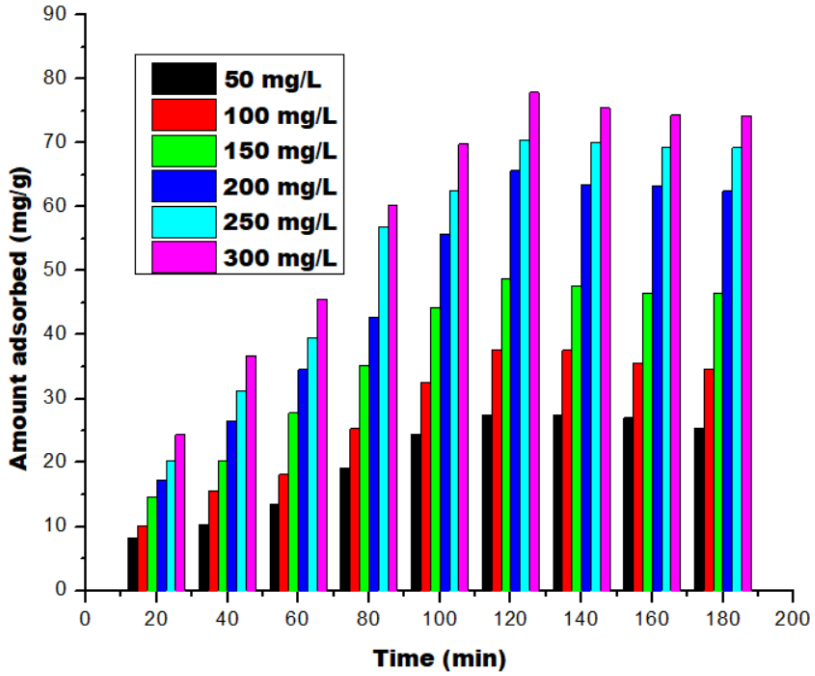

Fig. 5. Contact time impact and pollutant concentration's role on the sorption of CR using HWTCW

The concentration of pollutants is vital in determining the adsorption performance of an adsorbent material. Because adsorption is a surface phenomenon, the interaction between the adsorbent and the pollutant depends heavily on the concentration of the pollutants in the solution. When the role of the pollutant concentration was assessed, it was observed that for CR, the amount removed surged from 27.4 to 77.9 mg/g when the pollutant concentration was raised from 50 to 300 mg/L, whereas the amount of Cr (VI) adsorbed surged from 23.9 to 69.7 mg/g at the same pollutant concentration. Ofudje *et al.* (2022) observed that the concentration gradient between the pollutant in the solution and the adsorbent surface is the driving force for adsorption and that a higher concentration of pollutant provides a stronger driving force, leading to faster diffusion of pollutant molecules to the adsorbent surface.

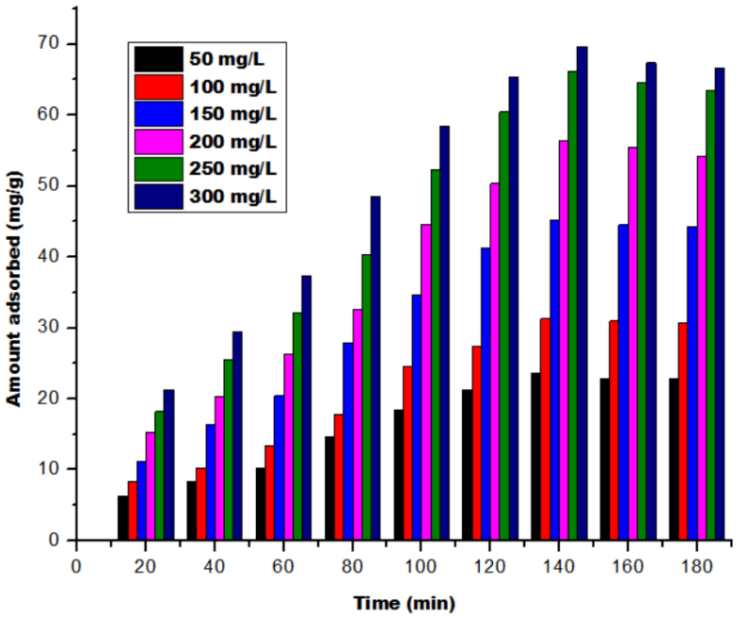

Fig. 6. Contact time impact and pollutant concentration's role on the sorption of Cr (VI) using HWTCW

Study on pH effect

The pH of the pollutant solution is a crucial factor influencing the adsorption process. Figure 7 shows that as the pH rose from 2 to 5, the percentage removal of cresol red rose from 56.2% to 76.5%. For Cr (VI) ions, the amount of removal increased sharply from 52.3% to 70.3% when the pH was adjusted from 2 to 3. Data from the point of zero charge (PZC) tests revealed that the hot water-modified cow waste had a PZC value of 3.9. The PZC, or isoelectric point, is critical for determining the surface charge of an adsorbent. Typically, when the solution's pH is higher than the PZC, the adsorbent is more effective at adsorbing positively charged pollutants (Ofudje *et al*. 2022). Conversely, when the pH is below the PZC, the adsorbent is more suited to adsorbing negatively charged contaminants. A uniformly negative surface charge above the PZC implies that the sawmill wood waste adsorbent has a heterogeneous surface, containing both amine groups (which remain positively charged up to pH of 9) and carboxylate groups (which are negatively charged below pH 2). This implies that even at pH 6 (above the PZC), some localized positive charges may still exist, allowing electrostatic attraction with the anionic Crystal Red dye. Thus, adsorption is not solely dependent on electrostatic interactions but also influenced by surface heterogeneity, hydrogen bonding, and π–π interactions with lignin. Shabiimam and Ani (2012) observed that in the adsorption of o-cresol by landfill leachate, maximum adsorbate removal was achieved at a pH of 8. In a literature report by Herbache *et al*. (2015), it was noticed that the uptake of o-cresol surged with pH and that maximum adsorption was attained at pH of 6.31 and thereafter it showed a significant decline within basic pH. They based their argument on the fact that because the PZC value of the adsorbent used is 5.1 and that the pKa of o-cresol is 10.3, it is expected that within this pH range, the o-cresol will only exist in the molecular form, which is basic in nature due to the electron releasing groups of methyl and hydroxyl. They explained further that because the surface of the adsorbent has a net positive charge with PZC of 5.11, there is a high adsorption uptake due to a more affinity for the molecular form of o-cresol (Herbache *et al.* 2015). In contrast, Cr(VI) exists in

various forms depending on the solution pH. Under acidic conditions (low pH), Cr(VI) primarily exists as $HCrO_4^-$ (hydrogen chromate ions) and $Cr_2O_7^{2-}$ (dichromate ions), while at higher pH (alkaline conditions), it predominantly exists as CrO_4^{2-} (chromate ions). The dominant species at low pH is $HCrO_4^-$, which is more easily adsorbed onto positively charged surfaces. Lower pH levels enhance Cr(VI) adsorption due to the formation of favorable species such as $HCrO_4^-$ and the presence of a positively charged adsorbent surface. In contrast, higher pH reduces adsorption due to repulsion between the negatively charged adsorbent and the more negatively charged Cr(VI) species CrO_4^{2-}. Shi *et al*. (2020) documented a maximum adsorption capacity of 620 mg/g at pH 2.0, attributing this to the specific chromium species present and the surface charge on a lignin-based composite. They explained that under acidic conditions, protonation of the amino groups resulted in positive charges on the surface, thus enhancing adsorption through electrostatic attraction. Similarly, Misbah *et al*. (2016) reported a maximum Cr(VI) adsorption capacity of 85.6 mg/g at pH 3 when using a mango biocomposite, ascribing this to changes in Cr(VI) species and surface charges of mango biocomposite.

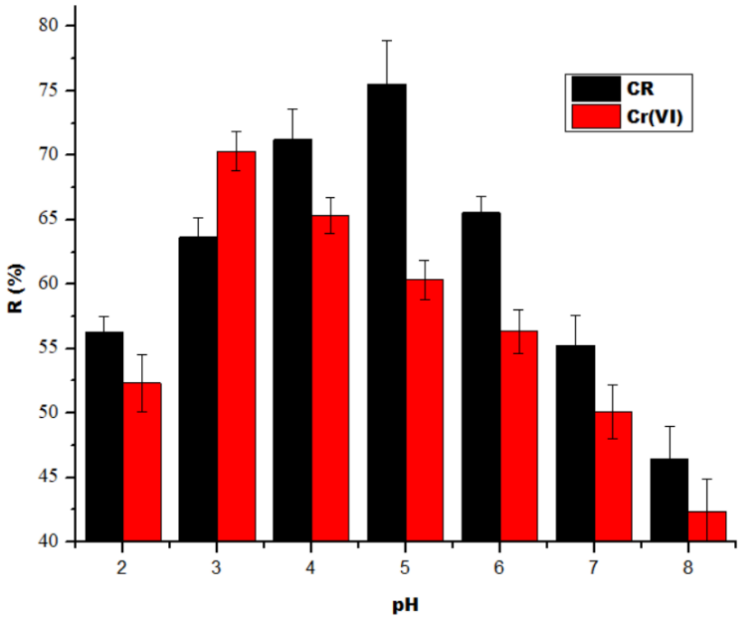

Fig. 7. pH's effect on the adsorption of cresol red and hexavalent chromium using hot water-modified cow waste

At lower pH, the surface of the material is likely to have a net positive charge due to the presence of any amine functions, and this will favor negatively charged $HCrO_4^-$ ions species through electrostatic attraction, leading to increased adsorption efficiency. On the other hand, higher pH values (less acidic) might favor higher concentrations of the negatively charged species of fatty acids in solution, and the cresol red dye being a strong acid, might experience enhanced adsorption. El Kassimi *et al.* (2023) also observed maximum efficiencies of 85.9% and 96% for Cr (VI) adsorption at pH 1.5 using *medlar* and *Cucumis melo* activated carbons, respectively. A decrease in adsorption capacity was noted when the pH increased from 1.5 to 4.0, which they attributed to electrostatic forces caused by the positively charged adsorbent surface because of protonated functional groups and the dominance of $HCrO_4^-$. Islam (2018) similarly reported that birnessite's sorption capacity for Cr (VI) adsorption depends highly on solution pH, as maximum sorption was seen at pH of 2.0, linking this to the anionic nature of hexavalent chromium

species and the adsorbent's positively charged surface. Overall, Cr (VI) and cresol red dye sorption by hot water-treated cow waste occurred primarily through electrostatic forces.

Reduction of Cr(VI) to Cr(III)

The reduction of hexavalent chromium (Cr(VI)) to trivalent chromium (Cr(III)) during adsorption using cow dung manure involves both chemical and surface-mediated processes. Cow dung manure contains various organic compounds and functional groups such as -OH, C=O, C=C, and C-O that can act as electron donors (reducing agents), reducing Cr(VI) to Cr(III) and facilitate this redox transformation (Das *et al*. 2000; Wu *et al*. 2017).

The reduction mechanisms can be represented by the following simplified reactions:

Adsorption of Cr(VI):

$$Cr_2O_7^{2-} + S \rightarrow S\text{-}Cr_2O_7^{2-}$$

In this expression, S stands for the surface of the adsorbent, and herein, dichromate ions ($Cr_2O_7^{2-}$) are adsorbed onto the surface of the cow dung-derived adsorbent.

Reduction to Cr(III):

$$S\text{-}Cr_2O_7^{2-} + RFG\ \text{(-OH, C=O, C=C or C-O)} \rightarrow S\text{-}Cr^{3+} + RFG$$

In this expression, RFG are the oxidized functional groups. In this second step, the reducing functional groups (*e.g.*, -OH, C=O, C=C or C-O) donate electrons to the adsorbed Cr(VI), reducing it to Cr(III), which remains bound to the surface. Thus, cow manure, with its rich organic content and functional groups, serves as an effective adsorbent for the removal of Cr(VI) from aqueous solutions in which the process involves the adsorption of Cr(VI) onto the adsorbent surface, followed by its reduction to the less toxic Cr(III) state, facilitated by the reducing functional groups present in the manure. This dual mechanism of adsorption and reduction underscores the potential of cow dung manure as a low-cost and eco-friendly material for treating chromium-contaminated water. Liang *et al*. (2018) observed few changes in the functional groups that took place after chromium ions were adsorbed on the surface of lignin-PEI adsorbent, and it was concluded that these functional groups contributed electrons and were oxidized during the reduction process of Cr(VI) to Cr(III). They thereafter established that the surface of lignin-PEI first adsorbed the anionic Cr(VI) through electrostatic attraction, complexation and possibly ion exchange and that as the adsorption proceeded, some of the Cr(VI) ions get reduced to Cr(III) ions *via* the redox reaction of neighboring electron-donor groups.

Adsorption Isotherm Studies

Isotherms are commonly used to represent adsorption processes that illustrate how the adsorbed molecules are distributed between the liquid and solid phases at equilibrium (Geçgel *et al.* 2013). Isotherms are mathematical tools for evaluating the efficiency of adsorbents in pollutant solutions by optimizing surface properties and adsorption capacity, thereby assessing the effectiveness of the adsorption system. To this end, Dubinin-Radushkevich (D-R), Langmuir, and Freundlich models were selected. The

Langmuir isotherm model assumes a homogeneous adsorbent surface, characterized by uniformly available active sites, monolayer adsorption, and consistent adsorbent-adsorbate interactions (Arica *et al.* 2004; Geçgel *et al.* 2013). In contrast, the empirical Freundlich isotherm model accounts for surface heterogeneity (Adeogun *et al.* 2012; Geçgel *et al.* 2013). As for the Dubinin-Radushkevich (D-R) model, it is primarily used to describe the adsorption process in microporous materials, particularly when physical adsorption rather than chemical adsorption is dominant. The D-R model helps in determining the nature of the adsorption process, such as whether it follows a physisorption mechanism and in assessing the porosity and surface properties of adsorbents. It differs from other isotherms like Langmuir and Freundlich in that it is based on a Gaussian distribution of adsorption energy rather than assuming a uniform energy of adsorption sites. The equations of these isotherm models are shown in equations 3 to 5 (Adeogun *et al.* 2012; Geçgel *et al.* 2013; Ofudje *et al.* 2023), while their variable values as obtained from Fig. 8 to Fig. 10 are listed in Table 1.

Dubinin–Radushkevich isotherm $$Inq_e = Inq_m - \beta\epsilon^2 \quad (3)$$

Langmuir: $$C_e / q_e = C_e/q_{max} + 1 / (q_{max}K_L K_L) \quad (4)$$

Freundlich: $$Inq_e = InK_F - \frac{1}{n}InC_e \quad (5)$$

In the Langmuir model, C_e is the equilibrium concentration of adsorbate (mg/L), q_{max} is the maximum adsorption capacity (mg/g) and K_L is the Langmuir constant (L/mg). The plot of C_e/q_e versus C_e was used to determine the various constants from the data obtained from the slope and the intercept, as depicted in Fig. 8. For the Freundlich model, q_e and C_e are as previously defined, K_F is the Freundlich constant that indicates adsorption capacity, and n is the adsorption intensity (dimensionless). The plot of $\ln q_e$ versus $\ln C_e$ was employed to compute the various constants from the slope and the intercept, as provided in Fig. 9. When n >1, it is favorable adsorption, n = 1 implies linear adsorption, and when n < 1, it is unfavorable adsorption. From D-R model, q_e denotes the amount of adsorbate adsorbed (mg/g), q_m is maximum adsorption capacity (mg/g), β (beta) represents the adsorption energy constant (mol^2/kJ^2), and ε represent the Polanyi potential. The plot of $\ln q_e$ against ε^2 was used to compute the various constants using the slopes and intercepts (Fig. 10).

Table 1. Physical Variables of Isotherms Models for the Adsorption of CR and Cr (VI) by HWTCW

	Parameters	CR	Cr (VI)
Langmuir	Q_{max} (mg/g)	74.33	66.42
	R_L	0.18	0.32
	b (mg/L)	0.104	0.079
	R^2	0.979	0.967
Freundlich	K_F (mg/g)(mg/L)$^{-1/2}$	44.34	35.84
	1/n	0.276	0.350
	R^2	0.966	0.989
Dubinin-Radushkevich	Q (mg/g)	55.27	46.21
	ε (molJ^{-1})^2	0.287	0.261
	E (kJmol^{-1})	6.34	11.225
	R^2	0.996	0.976

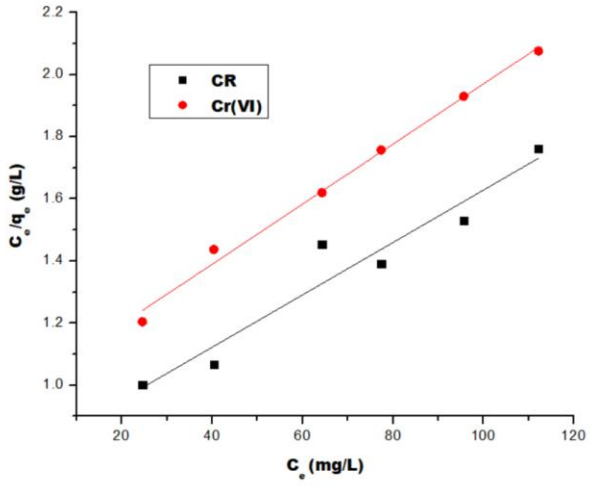

Fig. 8. Langmuir isotherm model for cow waste adsorbent for the adsorption of CR and Cr (VI)

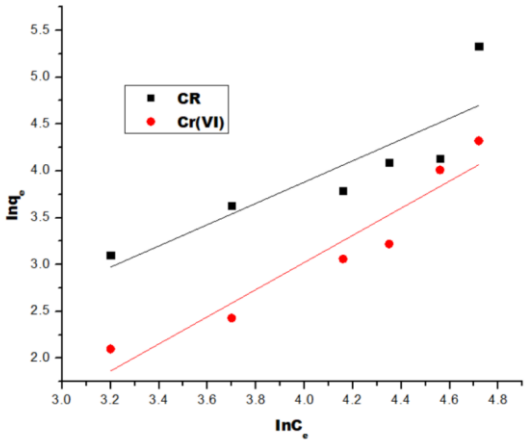

Fig. 9. Freundlich isotherm model for cow waste adsorbent for the adsorption of CR and Cr (VI)

The constant known as the Langmuir separation factor R_L was estimated using Eq. 6,

$$R_L = \frac{1}{(1+bC_o)} \quad (6)$$

where C_0 is the initial concentration of adsorbate and R_L indicates favorability with: $0<R_L<1$: Favorable adsorption, $R_L = 1$: Linear adsorption, and $R_L > 1$: Unfavorable adsorption.

From the D-R model, the Polani potential, which is expressed as ϵ in mol^2/j^2, is given as Eq. 7,

$$\in = RTIn(1+\frac{1}{C_e}) \quad (7)$$

where R is the universal gas constant with value of 8.314 J/mol·K and T is the temperature in Kelvin (K).

The adsorption free energy that is represented as E (kJ/mol) is mathematically represented as Eq. 8,

$$E = \frac{1}{\sqrt{2K_{DR}}} \quad (8)$$

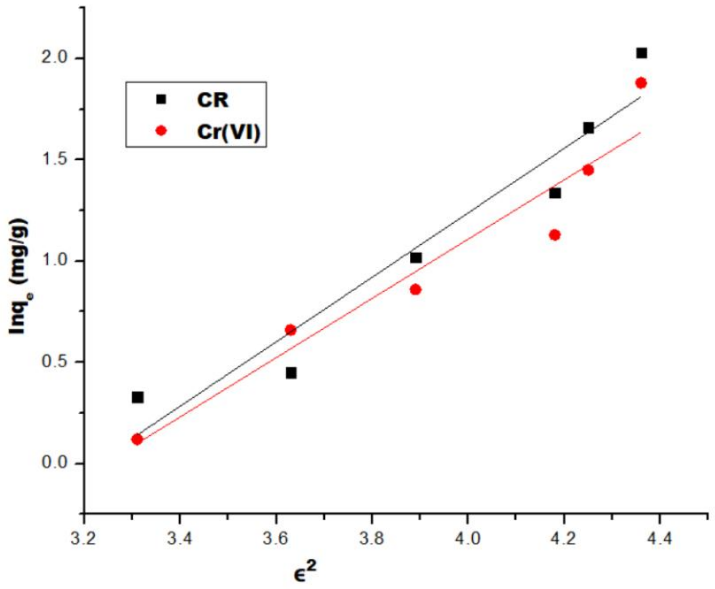

Fig. 10. Dubinin-Radushkevich (D-R) isotherm model for cow waste adsorbent for the adsorption of CR and Cr (VI)

From the information obtained, the maximum adsorption capacity of the hot water-treated cow waste adsorbent showed a higher capacity for cresol red (q_m = 74.3 mg/g) than for Cr(VI) (q_m = 66.4 mg/g. These determinations were corroborated by the coefficient of determination values (R^2 = 0.979 for CR) and (R^2 = 0.967 for Cr (VI)), indicating how well the Langmuir isotherm fit the experimental data of both adsorbates, with cresol red showing a marginally better fit to the model. Similarly, from the value of R_L = 0.180 for CR and R_L = 0.320 for Cr (VI), it indicates that the biomass had a higher favorability for the cresol red than Cr(VI) adsorption. This suggests a stronger interaction between the adsorbent and cresol red than the Cr(VI). From the Freundlich isotherm, the K_F value indicates a relatively higher adsorption tendency for cresol red (44.3 $(mg/g)(mg/L)^{-1/2}$) than for Cr (VI) (35.8 $(mg/g)(mg/L)^{-1/2}$), meaning that the adsorbent can adsorb a significant amount of cresol red at low equilibrium concentrations when compared with hexavalent chromium molecules. The value of $1/n$ was less than 1, indicating favorable adsorption. A higher $1/n$ indicates weaker interactions between the adsorbate and the adsorbent compared to cresol red. Furthermore, the marginally higher R^2 suggests that Cr(VI) adsorption is better modeled by the Freundlich isotherm, which could imply a more heterogeneous surface or varying adsorption sites.

Table 2. Comparable Analysis of Adsorption Capacities from Other Adsorbents Towards CR and Cr (VI) Uptake

Adsorbents	**Adsorption Capacities (mg)**	**References**
CR		
Activated carbon	27.78	Shabiimam and Anil (2012)
Sodium natural bentonite	58.824	Taleb *et al.* (2021)
Wastepaper	16.7	Salman *et al*. (2022)
β-CD/chitosan resin	39.9	Chen *et al*. (2006)
Cyclodextrin-based polymer	15.1	Peñas *et al*. (2022)
Al_2O_3/carbon nanotubes	70.4	Jaafari *et al*. (2018)
Synthetic hydroxyapatite	67.6	Zhu and Kolar (2016)
Hot water-treated cow waste	74.33	This study
Cr (VI)		
Sodium lignosulfonate	57.7	Liang *et al*. (2013)
Rice husk carbon	38.1	Singh *et al*. (2012)
Paper mill sludge	23.2	Gorzin and Bahri (2018)
Banana (*Musa cavendishii*) peel (BP)	10.4	Parlayici and Pehlivan (2019)
Montmorillonite-supported magnetite nanoparticles	20.16	Mthombeni *et al*. (2015)
Cucumis melo activated	54.28	El Kassimi *et al*. (2023)
Medlar activated carbon	34.12	El Kassimi *et al*. (2023)
Ocimum americanum L. seed pods	83.33	Yogeshwaran and Priya (2017)
Hot water-treated cow waste	66.42	This study

From the examination of the Dubinin–Radushkevich model, it was observed that the R^2 value of the cresol red dye (0.996) was higher than the hexavalent chromium ions (0.976), which means that the D-R isotherm model provides can be used to describe both CR and hexavalent chromium ions adsorption. The mean free energy values of 6.34 and 11.2 kJ/mol were obtained for CR and Cr(VI). The value for Cr(VI) was greater than 8 kJ/mol, which sometimes is taken as an indication of chemisorption, while a value less than 8 kJ/mol as observed for CR can be regarded as an indication of physisorption. The maximum adsorption capacity (q_m) for cresol red was 55.3 mg/g, which was higher than that of Cr(VI) with q_m of 46.2 mg/g, and this further suggests that the adsorbent for cresol red had a higher capacity to adsorb the substance when compared with Cr(VI) ions. Table 2 shows that the present adsorbent (HWTCW) performed excellent when compared with other documented adsorbents in the literature. Generally, the analysis did not provide

sufficient evidence to reject any of the three adsorption isotherm models viz: Langmuir, Freundlich, and Dubinin–Radushkevich, as they all gave suitable representations of the data, and each model adequately described the adsorption behavior observed in the study.

Since HWTCW exhibited great adsorption capacities comparable to and even in some cases exceeding existing values, it positions itself as a competitive alternative for contaminant removal. Its advantages include low cost, abundance, and sustainability, which are crucial for large-scale applications. HWTCW's low-cost nature can offset slightly lower adsorption capacities compared to high-performance adsorbents such as specialized activated carbons, while the feasibility of regenerating and reusing HWTCW without significant loss in capacity enhances its practical appeal as well. Thus, utilizing agricultural waste like HWTCW aligns with sustainable practices, reducing environmental footprints associated with adsorbent production.

Adsorption kinetic studies

The adsorption process is influenced by both the physical and chemical properties of the adsorbent system, as well as the specific conditions under which adsorption occurs. In this study, pseudo-first-order (PFO), pseudo-second-order (PSO), and intraparticle diffusion kinetics were examined. The equations for these kinetic models are presented in equations 9 to 11 (Adeogun *et al.* 2012; Geçgel *et al.* 2013; Ofudje *et al.* 2023). A comparative analysis of PFO and PSO kinetics was conducted, evaluating performance based on parameters, such as experimental and calculated adsorption capacities, and rate constants (k_1 and k_2), as shown in Tables 3 and 4 using Fig. 11 to 13.

Pseudo-first-order: $$In(q_e - q_t) = Inq_e - k_1 t \quad (9)$$

Pseudo-second-order: $$t / q_t = 1 / (k_2 q_e^2) + t / q_e \quad (10)$$

Intra-particle diffusion: $$q_t = K_p t^{1/2} + C_i \quad (11)$$

The best fit was determined from the coefficient of determination (R^2) values and also the sum of error squares (SSE, %) (Ofudje *et al.* 2020):

$$\% \text{ SSE} = \sqrt{\frac{((Q_{(exp)} - Q_{(Cal)})/Q2_{exp}}{N - 1}} \quad (12)$$

where q_t and q_e are the amount of adsorbate adsorbed at time t and at equilibrium (mg/g). k_1 and k_2 are the pseudo-first-order rate constant (min^{-1}) and pseudo-second-order rate constant (g/mg·min) respectively, and t is time (min). In the case of the plot of $\ln(q_e - q_t)$ against t was used to deduce the values of the constants from slope and intercept of the plot (Fig. 11), whereas for the second-order model, the plot of t/q_t against t was used for the variable determination *via* the slope and intercept as shown in Fig. 12. For the intraparticle diffusion model, q_t, and t are as defined previously, k_p is the intraparticle diffusion rate constant ($mg/g \cdot min^{0.5}$) and C_i denotes the constant that relates to boundary layer thickness. On plotting q_t against $t^{0.5}$, the variables were evaluated (Fig. 13).

For cresol red adsorption by HWTCW, the PFO kinetic model provided a better match to the experimental adsorption capacity, with calculated values closer to the experimental ones compared to the PSO model. The rate constants ranged from 0.153 to 0.461 for PFO (k_1) and from 0.131 to 1.050 for PSO (k_2), with a more significant variation observed in k_2. This indicates that the adsorption process is more sensitive to

changes in conditions under second-order kinetics. The PFO model demonstrated a better fit, as evidenced by higher R^2 values, which indicate a closer correlation to the experimental data. Additionally, lower %SSE values in the PFO model suggest minimal error between experimental and calculated values, making it a more accurate model compared to the PSO model, which had higher %SSE.

In contrast, for Cr(VI) adsorption by HWTCW, the PSO model provided a closer match between the experimental and calculated adsorption capacities. The smaller difference between these values, along with higher R^2 values and lower %SSE for PSO kinetics, suggests that this model more accurately represents the adsorption behavior for Cr(VI). The PSO model showed a better fit to the experimental data with fewer errors in prediction. Thus, for cresol red adsorption, PFO kinetics is the better model, while for Cr(VI) adsorption, PSO kinetics offers a more accurate representation. This finding is consistent with the observations of Misbah *et al*. (2016) and Iqbal *et al*. (2013), who also reported that Cr(VI) adsorption followed the PSO kinetic model.

In the comparative analysis of intra-particles diffusion mechanism, the performance of each adsorption process was analyzed based on the diffusion rate constant (k_p), intercept value (C_1), and coefficient of determination (R^2), as depicted in Tables 3 and 4. The higher k_p values for cresol red adsorption (5.325 to 34.553) suggest a faster diffusion process compared to Cr(VI) adsorption (2.355 to 17.227). This implies that cresol red molecules diffused more quickly into the pores of the cow waste adsorbent than Cr(VI) ions. The greater range of k_p values for cresol red also suggests more variability in the adsorption rates across different conditions or concentrations. The intercept value C_1 represents the thickness of the boundary layer, with a higher value indicating a greater contribution from surface adsorption. For cresol red, C_1 was higher, ranging up to 4.226, compared to Cr(VI), where the maximum C_1 was 2.035. This indicates that surface adsorption played a more significant role in cresol red adsorption than in Cr(VI) adsorption, suggesting that cresol red adsorbs more on the surface before intra-particle diffusion takes place. Both adsorption processes showed high R^2 values, indicating that intra-particle diffusion was a good model for describing the adsorption behavior of the two pollutants.

The intraparticle diffusion kinetic model explains the transport of adsorbate molecules from the bulk solution into the internal pores of a porous adsorbent. The process begins with an external mass transfer, or film diffusion, where adsorbate molecules migrate from the bulk solution to the adsorbent's external surface through a surrounding boundary layer. In the second stage, intraparticle diffusion occurs as the adsorbate moves into the internal pore network, which is often the rate-limiting step in adsorption. Finally, in the third stage, adsorption onto active sites takes place, where the adsorbate molecules attach to specific sites within the internal structure of the adsorbent (Ofudje *et al*. 2024a).

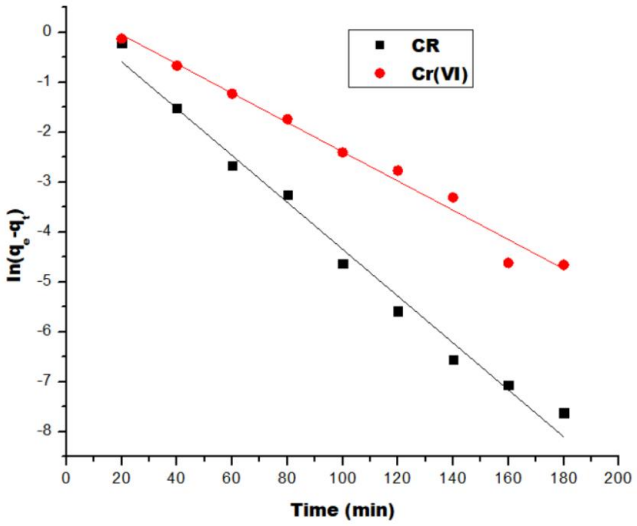

Fig. 11. PFO kinetics plots of the adsorption of hexavalent chromium ions and cresol red dye by HWTCW

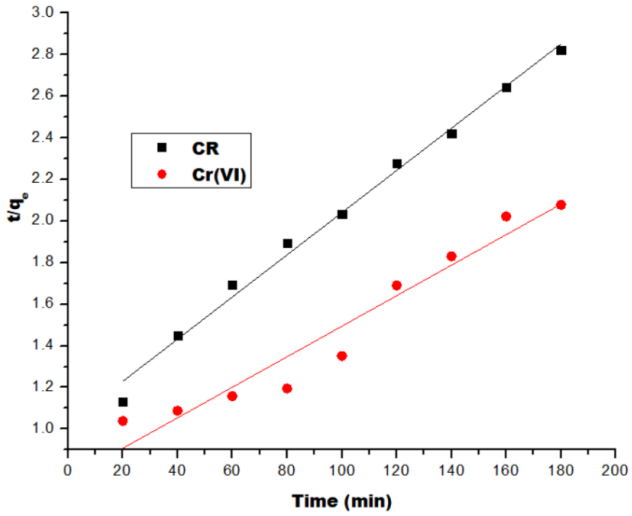

Fig. 12. PSO kinetics plots of the adsorption of hexavalent chromium ions and cresol red dye by HWTCW

Table 3. Constants From Kinetics Models for the Adsorption of Cresol Red by HWTCW

		First Order				Second Order				Intra Particle Diffusion		
C_o (mg/L)	$Q_{e(exp)}$ (mg g^{-1})	$Q_{e\ cal}$ (mg g^{-1})	k_1 (min^{-1})	R^2	% SSE	$Q_{e\ cal}$ (mg g^{-1})	k_2 (g mg^{-1} min^{-1})	R^2	% SSE	Kp (mg g^{-1} $min^{-0.5}$)	C_1 (mg g^{-1})	R^2
50	27.441	28.022	0.153	0.988	0.009	24.524	0.131	0.919	0.043	5.325	0.156	0.966
100	37.632	38.251	0.182	0.976	0.007	31.221	0.353	0.942	0.070	9.663	0.663	0.958
150	48.836	47.624	0.216	0.985	0.010	42.651	0.673	0.951	0.052	12.895	1.062	0.976
200	65.630	67.210	0.260	0.994	0.010	58.564	0.881	0.924	0.044	16.055	1.225	0.977
250	70.440	69.460	0.330	0.979	0.006	65.262	0.942	0.933	0.030	19.431	2.315	0.987
300	77.872	78.021	0.461	0.988	0.001	71.223	1.050	0.889	0.035	34.553	4.226	0.984

Table 4. Constants from the Kinetics Models for the Adsorption of Cr (VI) by HWTCW

		First Order				Second Order				Intra Particle Diffusion		
C_o (mg/L)	$Q_{e(exp)}$ (mg g^{-1})	$Q_{e\ cal}$ (mg g^{-1})	k_1 (min^{-1})	R^2	% SSE	$Q_{e\ cal}$ (mg g^{-1})	k_2 (g mg^{-1} min^{-1})	R^2	% SSE	Kp (mg g^{-1} $min^{-0.5}$)	C_1(mg g^{-1})	R^2
50	23.630	26.144	0.224	0.955	0.043	24.225	0.245	0.997	0.010	2.355	0.105	0.976
100	31.330	35.215	0.463	0.975	0.051	31.101	0.553	0.997	0.003	5.322	0.225	0.954
150	45.270	40.214	0.735	0.944	0.046	46.051	0.822	0.989	0.007	7.332	0.618	0.963
200	56.430	50.225	1.224	0.965	0.045	58.011	1.042	0.996	0.011	10.288	1.266	0.977
250	66.141	69.331	1.638	0.972	0.020	67.204	1.227	0.996	0.007	13.301	1.638	0.946
300	69.670	73.446	2.335	0.966	0.022	71.141	1.553	0.998	0.009	17.227	2.035	0.966

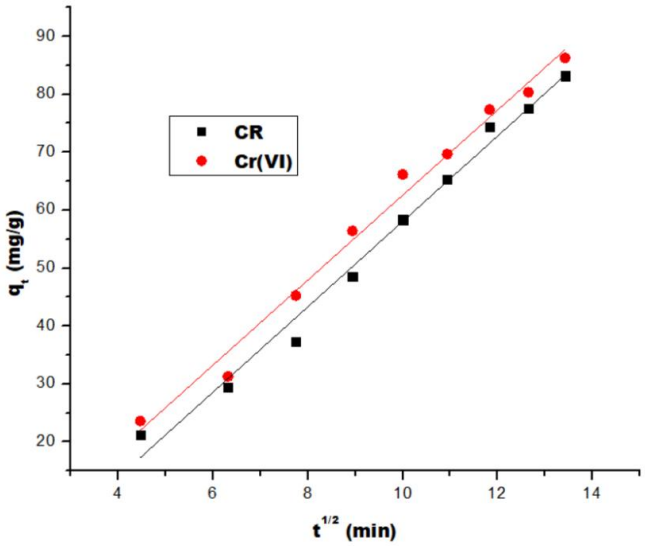

Fig. 13. Intra-particles diffusion kinetics plots of the adsorption of hexavalent chromium ions and cresol red dye by HWTCW

Temperature impact and thermodynamic studies

The role played by temperature on the removal of Cr(VI) ions and CR from aqueous solution was studied by varying the temperature of the adsorption between 25 and 65 °C. Results are presented in Fig. 14. In the case of cresol red dye adsorption, at 25 °C, the adsorption capacity was 54.3% and as the temperature increased to 40 °C, the adsorption capacity rose to 79.9%, indicating an improvement of about 47.0% from the initial value. However, at 65 °C, the adsorption capacity dropped to 60.3%, marking a 24.5% decrease from its peak value at 40 °C. On the examination of the effect of temperature on hexavalent chromium ion adsorption at 25 °C, the adsorption capacity was 48.3%. With an increase in temperature to 45 °C, the adsorption efficiency reached 75.4%, reflecting a rise of approximately 56.1%. Further increase to 65 °C resulted in a drop in adsorption capacity to 55.4%, representing a 26.5% decrease from its peak value at 45 °C. This is could be due to increased kinetic energy, which enhances molecular interactions and the diffusion rate of dye molecules to the active sites of the cow waste adsorbent. The decrease in adsorption capacity at elevated temperature likely reflects desorption or weakening of bonds.

In addition, at elevated temperatures, the formation of emulsions mixtures where tiny droplets of one liquid are dispersed within another becomes more pronounced and this increase in emulsified matter can trap pollutants within the dispersed droplets, effectively keeping them in a state similar to being dissolved in the liquid phase rather than allowing them to adsorb onto solid surfaces. As a result, the pollutants remain in the liquid phase, reducing their availability for adsorption onto solid adsorbents. This phenomenon can lead to a decrease in the efficiency of processes designed to remove pollutants through adsorption, as the emulsified state hinders the transfer of pollutants from the liquid to the solid phase. Also, elevated temperatures enhance the reduction of hexavalent chromium (Cr(VI)) to trivalent chromium (Cr(III)) and subsequently reducing the amount of Cr (VI) in the media

For cresol red dye, maximum adsorption occurred at 40 °C, while for hexavalent chromium ions, maximum adsorption occurred at 45 °C. According to Misbah *et al.* (2016), biosorption capacity was reduced when the temperature was increased and that the rate constant equally dropped with rise in temperature, thus indicating the adsorption of Cr(VI) to be exothermic in nature. They observed that with higher temperature, the mobility of the pollutant's molecules is accelerated and could cause desorption of these molecules but at low temperature, these molecules could efficiently adsorb onto the surface of the adsorbent. However, this report is contrary to the findings of the current study, which is found to be in agreement with the reports of El Kassimi *et al*. (2023), where it was recorded that as the temperature increases from 25 to 55 °C, the adsorption capacity of Cr (VI) by *medlar* activated carbon and *Cucumis melo* activated carbon also increased and that the amount of Cr (VI) adsorbed rose from 33.2 to 37.1 mg/g and from 48 to 54.6 mg/g, respectively. They explained that this phenomenon is caused by the increase in the mobility of Cr(VI) molecules in solution, which enhances their migrations to active adsorption sites.

In the current study, both pollutants showed a peak adsorption capacity at relatively moderate temperatures, suggesting the cow waste adsorbent has an optimal temperature range for adsorption. The adsorption capacity for cresol red dye shows a greater fluctuation with temperature changes, dropping from 79.9% to 60.3% between 40 and 65 °C, indicating that the dye adsorption process might be more sensitive to temperature changes compared to hexavalent chromium ions. Hexavalent chromium ions showed a more gradual decline from 75.4% to 55.4%, suggesting a relatively more stable adsorption mechanism over a wider temperature range.

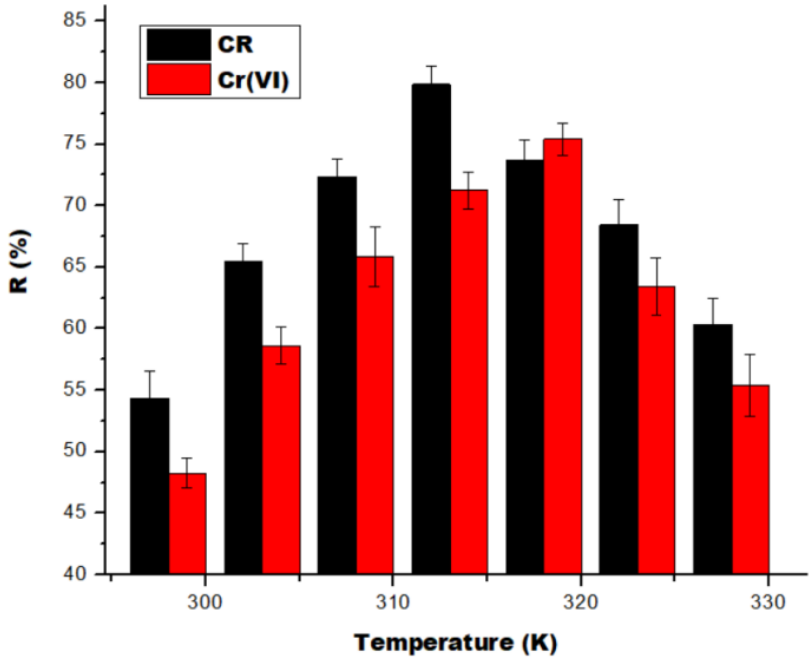

Fig. 14. Temperature impact on cresol red and Cr (VI) adsorption using cow waste

Thermodynamic variables such as the Gibbs free energy change (ΔG), enthalpy change (ΔH), and entropy change (ΔS) were evaluated, with the results presented in Table 4. According to thermodynamic analysis, ΔG is related to ΔH and ΔS at a given

temperature by the Van't Hoff equation (Adeogun *et al.* 2012; Ofudje *et al*. 2020), which is set out in Eqs. 13 through 15,

$$InK_C = -\frac{\Delta H^o}{RT} + \frac{\Delta S^o}{R} \quad (13)$$

$$K_C = \frac{q_e}{C_e} \quad (14)$$

$$\Delta G = -RTInK_C \quad (15)$$

where *K*c is the equilibrium constant representing the ratio of the amount adsorbed (q_e) in mg/g to the equilibrium concentration (C_e) in mg/L, and *R* is the molar gas constant.

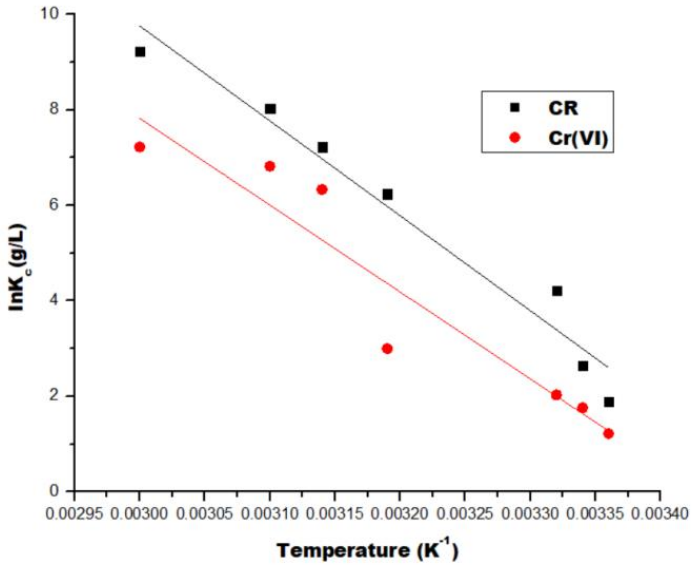

Fig. 15. Thermodynamic plots for the uptake of cresol red and Cr (VI) ions adsorption using cow waste

The relationship between Δ*G*, Δ*H*, and Δ*S* was determined from the linear plot of Δ*G* against the inverse of temperature (1/*T*), as shown in Fig. 15. The analysis of Δ*G* shows that the process of adsorption cresol red dye and hexavalent chromium ions was spontaneous at all temperatures studied, as Δ*G* was negative in both cases (Adeogun *et al*. 2012; Ofudje *et a*l. 2020). For cresol red, the adsorption became more spontaneous with increasing temperature (Δ*G* had increasing negative values as the temperature increased). For hexavalent chromium, the change in Δ*G* was less pronounced compared to cresol red, suggesting that the adsorption of cresol red was more spontaneous at elevated temperatures (338 K), as indicated by its increasingly negative Δ*G* values. At lower temperatures (298 K), both adsorption processes exhibited similar spontaneity levels. The positive enthalpy values (cresol red: Δ*H* = 22.4 kJ/mol; hexavalent chromium: Δ*H* = 46.0 kJ/mol) indicate the endothermic nature of the adsorption, with hexavalent chromium exhibiting a more endothermic process. This higher Δ*H* value suggests that the adsorption of hexavalent chromium requires more energy and involves stronger adsorbate-adsorbent interactions compared to cresol red (Ofudje *et al*. 2024b). In

industrial settings, maintaining elevated temperatures could improve removal efficiency, making the process more effective. Additionally, industries operating at elevated temperatures (*e.g.*, metal plating, dye manufacturing) can integrate HWTCW adsorption units without significant modifications to existing thermal conditions, enhancing Cr(VI) removal efficiency without incurring extra heating costs.

Positive Δ*S* (cresol red: Δ*S* = 5.16 J/mol·K and hexavalent chromium: Δ*S* = 10.3 J/mol·K) in both cases suggest an increase in disorder at the solid-liquid interface during adsorption (Uzosike *et al*. 2022). However, the entropy change for hexavalent chromium was higher, indicating a more significant increase in disorder in the system compared to cresol red. This could imply that the chromium ions displace more water molecules or undergo greater structural reorganization upon adsorption compared to cresol red molecules.

Table 4. Thermodynamic Constants for Adsorption of Cr (VI) and Cresol Red Dye Using Cow Waste

T (K)	Δ*G*	Δ*H*	Δ*S*	Δ*G*	Δ*H*	Δ*S*
	Cresol Red			**Hexavalent Chromium Ions**		
298	-0.660			-0.142		
303	-1.252			-0.621		
308	-1.543	22.430	5.162	-1.023	46.035	10.251
313	-2.245			-1.130		
318	-2.451			-1.873		
328	-3.252			-2.254		
338	-3.730			-2.942		

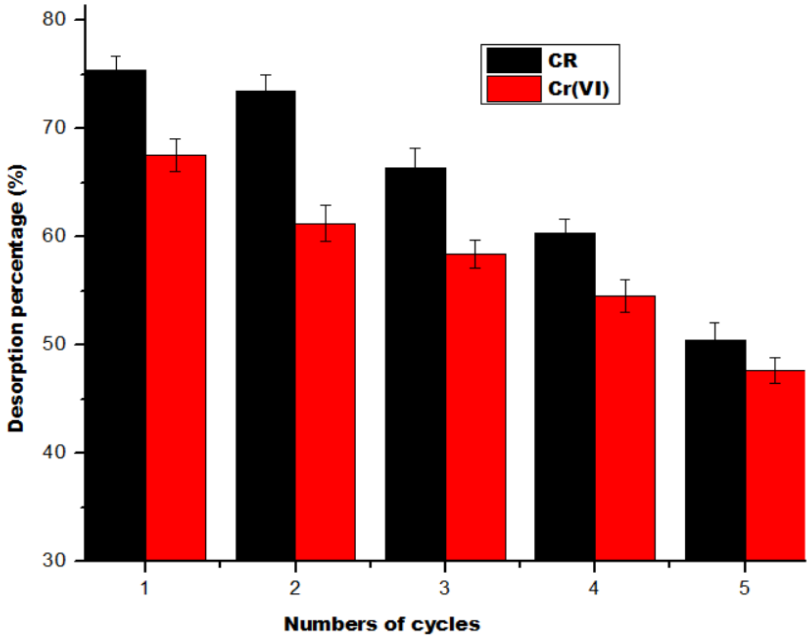

Fig. 16. Regeneration study of HWTCW

Regeneration Evaluation

To evaluate the regeneration capacity of the biomass, the already used HWTCW was treated with 0.1 M HCl followed by distilled water to remove the pollutant from the surface. The desorption process was carried out for 120 min by reconstituting the adsorbent inside an adsorbate solution and then agitating. After filtration, the pollutant concentration was measured and the desorption efficiency was estimated and the results are shown in Fig. 15. The desorption efficiency of the adsorbent showed a gradual decrease as the number of cycles increased, indicating good desorption ability. After five successive cycles, the desorption efficiency ranged from 54.2% to 75.3% for CR and from 46.3% to 68.4% for Cr(VI). Minimal changes were seen in the adsorption process after three cycles, attributed to slight reductions in the adsorption capacity of the adsorbent, particularly after the fifth cycle.

ADSORPTION MECHANISM

The functional groups present on the surface of hot water-treated cow waste (HWTCW), particularly hydroxyl (-OH) and carbonyl (C=O) groups, play a crucial role in the adsorption of Cr(VI) and Cresol Red from aqueous solutions. Also, since the adsorption of CR and Cr (VI) perfectly fits this model, it suggests that diffusion within the adsorbent pores is a key part of the adsorption mechanism process. However, the intraparticle diffusion occurs in conjunction with surface adsorption kinetics, indicating that adsorption isn't controlled by a single mechanism but rather by a combination of film diffusion, surface interactions, and pore diffusion.

Interaction with Cr(VI)

Cr(VI) typically exists in aqueous solutions as anionic species such as $HCrO_4^-$ (hydrogen chromate ions) and $Cr_2O_7^{2-}$ (dichromate ions) at lower solution pH as experienced in this study. The likely adsorption mechanisms could involve electrostatic interactions, complexation and most likely, potential redox reactions. In case of the electrostatic attraction, the -OH and C=O groups when protonized at lower pH could form positive charge on the HWTCW surface, which facilitates the attraction of the negatively charged Cr(VI) species. For complexation mechanism, the lone pairs of electrons on oxygen atoms in -OH and C=O groups can form coordination bonds with Cr(VI) ions, enhancing adsorption. While for redox reactions, the functional groups such as -OH may participate in redox reactions, reducing Cr(VI) to the less toxic Cr(III), which can then form stable complexes with the functional groups on the adsorbent surface.

Interaction with Cresol Red

Cresol red is an anionic dye with sulfonate groups that can interact with the functional groups on HWTCW through different reaction mechanisms. The adsorption of crystal red onto sawmill wood waste is influenced by both hydrophobic and hydrophilic interactions due to the dual nature of its molecular structure. The aromatic rings in crystal red facilitate π–π interactions with lignin, a major component of wood waste, while van der Waals forces further enhance adsorption and these non-polar interactions contribute significantly to the affinity of the dye for the wood waste surface (Han *et al*. 2022). In addition, the sulfonic ($-SO_3H$) and hydroxyl (-OH) functional groups in crystal red enable

hydrogen bonding with cellulose and hemicellulose in the wood waste. Electrostatic interactions also play a role, depending on the pH. At lower pH, the wood waste surface becomes more protonated, strengthening electrostatic attraction with the negatively charged sulfonate ($-SO_3^-$) groups of crystal red (Salahuddin *et al*. 2020). At higher pH, both the dye and the adsorbent acquire negative charges, leading to electrostatic repulsion, though hydrogen bonding and π–π interactions may still contribute to adsorption (Salahuddin *et al*. 2020). Overall, the adsorption mechanism is a combination of π–π interactions, hydrogen bonding, and pH-dependent electrostatic forces.

CONCLUSIONS

This work presents hot water-treated cow waste adsorbent as a cheap and effective adsorbent for the removal of cresol red and hexavalent chromium ions from aqueous solution. Specific findings from the study are listed below:

1. The results revealed that the adsorption efficiency of hot water-treated cow waste depends on the experimental conditions investigated.
2. Equilibrium data for the adsorption of cresol red dye and Cr (VI) conformed to the three isotherms tested *viz*: Freundlich, Langmuir and D-R models.
3. Based on the magnitude of free energy of adsorption, for cresol red the adsorption can be classed as physisorption, whereas the adsorption of Cr (VI) can be classed as chemisorption.
4. The presence of cellulose functional groups in the adsorbent played a key role in the adsorption process, based on shifts in FTIR spectra.
5. The cow waste proved to be more of an adsorbent for cresol red uptake compared to Cr(VI), indicating stronger interactions between the adsorbent and cresol red.
6. Hot-water-treated cow waste is an effective adsorbent for the removal of both cresol red dye and Cr(VI) ions from aqueous solutions.

ACKNOWLEDGMENTS

The authors express their gratitude to the Deanship of Scientific Research at Northern Border University, Arar, KSA, for funding this research work through the project number "NBU-FFR-2025-2985-03". We also appreciate Princess Nourah bint Abdulrahman University Researchers Supporting Project number (PNURSP2025R65), Princess Nourah bint Abdulrahman University, Riyadh, Saudi Arabia.

Conflict of Interest

No conflict of interest exists.

Data Availability

The datasets used and/or analyzed during the current study are available from the corresponding author on reasonable request.

REFERENCES CITED

Abayneh, K., Kassim, K., Fekadu, M., and Tsegaye, G. A. (2022). "Removal of Cr(VI) from aqueous solutions using biowastes: Tella residue and pea (*Pisum sativum*) seed shell," *The Sci. World J.* article 7554133. DOI: 10.1155/2022/7554133

Adeogun, A. I., Ofudje, E. A., Idowu, M. A., and Ahmed, S. A. (2012). "Biosorption of Cr(VI) ion from aqueous solution by maize husk: Isothermal, kinetic and thermodynamic study," *Journal of Chemical Society of Pakistan* 34(6), 1388-1396.

Adane, T., Haile, D., Dessie, A., Abebe, Y., and Dagne, H. (2020). "Response surface methodology as a statistical tool for optimization of removal of chromium (VI) from aqueous solution by teff (*Eragrostis teff*) husk activated carbon," *Applied Water Science* 10, article 37. DOI: 10.1007/s13201-019-1120-8

Alghamdi, A. A., Al-Odayni, A.-B., Saeed, W. S., Al-Kahtani, A., Alharthi, F. A., and Aouak, T. (2019). "Efficient adsorption of lead (II) from aqueous phase solutions using polypyrrole-based activated carbon," *Materials* 12(12), article 2020. DOI: 10.3390/ma12122020

Ali, A. G. K., Sohrab, A.G., Younes, A., and Mohammad, M. S. (2023). "Investigation of kinetic, isotherm and adsorption efficacy of thorium by orange peel immobilized on calcium alginate," *Sci. Rep*. 13, article 8393. DOI: 10.1038/s41598-023-35629-z

Ameer, B. K., and Mutah, M. (2015). "Cresol red dye removal using recycled waste tire rubber," *International Journal of Engineering Research in Africa* 16, 57-63.

Anuar, F. I., Hadibarata, T., Muryanto, Yuniarto, A., Priyandoko, D., and Arum, S. A. (2019). "Innovative chemically modified biosorbent for removal of procion red," *International Journal of Technology* 10, 776-786.

Arica, M. Y., Bayramoglu, G., Yilmaz, M., Bectas, S., and Genc, O. (2004). "Biosorption of Hg^{2+}, Cd^{2+} and Zn^{2+} by Ca-alginate and immobilized wood-rotting fungus, *Funalia trogii*," *Journal of Hazardous Materials B* 109, 191-199.

Ayyappan, T., and Elangovan, G. (2017). "Experimental study on removal of chromium by using cow dung as low cost adsorbents," *Int. J. Intell. Eng. and Syt.* 10(2). DOI: 10.22266/ijies2017.0430.02

Badr Khudhair, A., Musa, M., Mohd Jaafar, M. S., and Hadibarata, T. (2015). "Cresol red dye removal using recycled waste tire rubber," *Int. J. Eng. Res. in Africa* 16, 57-63. DOI: 10.4028/www.scientific.net/jera.16.57

Barot, N. S., and Bagla, H. K. (2012). "Eco-friendly waste water treatment by cow dung powder (Adsorption studies of Cr(III), Cr(VI) and Cd(II) using tracer technique)," *Desalin. and Water Treat.* 38(1-3), 104-113. DOI: 10.1080/19443994.2012.664309

Chen, Q. Y., Xiao, J. B., Chen, X. Q., Jiang, X. Y., Yu, H. Z.., and Xu, M. (2006). "The adsorption of phenol, *m*-cresol and *m*-catechol on a β-cyclodextrin derivative-grafted chitosan and the removal of phenols from industrial wastewater," *Adsorption Science & Technology* 24, 547-557. DOI: 10.1260/026361706780810230

Darmokoesoemo, H., Setianingsih, F. R., Putranto, T. W. L. C., and Kusuma, H. S. (2016). "Horn snail (*Telescopium* sp) and mud crab (*Scylla* sp) shells powder as low cost adsorbents for removal of Cu^{2+} from synthetic wastewater," *RASĀYAN J. Chem*. 9(4), 550-555.

Das, D. D., Mahapatra, R., Pradhan, J., Das, S. N., and Thakur, R. S. (2000). "Removal of Cr(VI) from aqueous solution using activated cow dung carbon," *Journal of Colloid and Interface Science* 232(2), 235-240. DOI:10.1006/jcis.2000.7141

Dawodu, F. A., Akpan, B. M., and Akpomie, K. G. (2020). "Sequestered capture and desorption of hexavalent chromium from solution and textile wastewater onto low cost *Heinsia crinita* seed coat biomass," *Applied Water Science* 10, 1-15. DOI: 10.1007/ s13201-019-1114-6

Delpiano, G. R., Tocco, D., Medda, L., Magner, E., and Salis, A. (2021). "Adsorption of malachite green and alizarin red S dyes using Fe-BTC metal organic framework as adsorbent," *International Journal of Molecular Sciences* 22, article 788. DOI: 10.3390/ijms22020788

El Kassimi, A., Aicha N., Hicham, Y., Youness, A., Abdelmajid, R., Mamoune, El H., Said, L., Rachid, L., and Mohammadine, El H. (2023). "Adsorption of chromium (VI) on low-cost adsorbents derived from agricultural waste material: A comparative study and experimental design," *International Journal of Environmental Analytical Chemistry* 2023, 1-23. DOI: 10.1080/03067319.2023.2200141

Elaigwu, S. E., Usman, L. A., Awolola, G. V., Adebayo, G. B., and Ajayi, R. M. K. (2009). "Adsorption of Pb(II) from aqueous solution by activated carbon prepared from cow dung," *Adv. Nat. Appl. Sci*. 3, 442-446.

Garba, J., Abd Samsuri, W., Othman, R., and Hamdani, M. S. A. (2019). "Evaluation of adsorptive characteristics of cow dung and rice husk ash for removal of aqueous glyphosate and aminomethylphosphonic acid," *Sci. Rep*. 9 (1), 1-10. DOI: 10.1038/s41598-019-54079-0

Geçgel, U., Ozcan, G., and Gürpınar, G. Ç. (2013). "Removal of methylene blue from aqueous solution by activated carbon prepared from pea shells (*Pisum sativum*)," *Journal of Chemistry* 2013, article ID 614083. DOI: 10.1155/2013/614083

Gorzin, F., and Bahri, R. A. M. (2018). "Adsorption of Cr (VI) from aqueous solution by adsorbent prepared from paper mill sludge: Kinetics and thermodynamics studies," *Adsorption Science & Technology* 36, 149-169. DOI: 10.1177/0263617416686

Guo, H., Li, H., Jing, C., and Wang, X. (2021). "Soluble polymers with intrinsic porosity for efficient removal of phenolic compounds from water," *Microporous and Mesoporous Materials* 319, article ID 111068. DOI: 10.1016/j.micromeso.2021.111068

Gupta, K. K., Aneja, K. R., and Rana, D. (2016). "Current status of cow dung as a bioresource for sustainable development," *Journal of Bioresources and Bioprocess Technology* 3, 1-11. DOI: 10.1186/s40643-016-0105-9

Han, X., Li, R., Miao, P., Gao, J., Hu, G., Zhao, Y., and Chen, T. (2021). "Design, synthesis and adsorption evaluation of bio-based lignin/chitosan beads for congo red removal," *Materials*, 15, 2310. DOI: 10.3390/ ma15062310

Herbache, H., Ramdani, A., Maghni, A., Taleb, Z., Taleb, S., Morallon, E., and Brahmi, R. (2015). "Removal of o-cresol from aqueous solution using Algerian Na-clay as adsorbent," *Desalination and Water Treatment* 57(43), 20511-20519. DOI: 10.1080/19443994.2015.1108240

Iqbal, J., Cecil, F., Ahmad, K., Iqbal, M., Mushtaq, M., Naeem, M., and Bokhari, T. (2013). "Kinetic study of Cr (III) and Cr (VI) biosorption using *Rosa damascena phytomass*: A rose waste biomass," *Asian Journal of Chemistry* 25, 2099-2103.

Ilyas, R. A., Sapuan, S. M., and Ishak, M. R. (2018). "Isolation and characterization of nanocrystalline cellulose from sugar palm fibres (*Arenga Pinnata*)," *Carbohydrate Polymer* 181, 1038-1051. DOI: 10.1016/j.carbpol.2017.11.045

Islam, M. A., Angove, M. J., and Morton, D. W. (2019). "Recent innovative research on chromium (VI) adsorption mechanism," *Environmental Nanotechnology, Monitoring and Management* 12, article ID 100267. DOI: 10.1016/j.enmm.2019.100267

Islam, M. A. (2018). *Competitive Sorption of Metal Ions and Humic Acid onto Manganese Oxides and Boehmite*, Ph.D. Thesis (Chemistry), La Trobe University, Melbourne, Victoria, Australia.

Jaafari, J., Ghozikali, M. G., Azari, A., Delkhosh, M. B., Javid, A. B., Mohammadi, A. A., Agarwal, S., Gupta, V. K., Sillanpää, M., Tkachev, A. G., and Burakov, A. E. (2018). "Adsorption of *p*-cresol on Al_2O_3 coated multi-walled carbon nanotubes: Response surface methodology and isotherm study," *Journal of Industrial and Engineering Chemistry* 57, 396-404. DOI: 10.1016/j.jiec.2017.08.048

Jana, A., El Malti, W., Luminita, D., Jacques, L., Al Ajami, M., Hussein, H., and Akram, H. (2024). 'Comparing conventional and advanced approaches for heavy metal removal in wastewater treatment: An in-depth review emphasizing filter-based strategies. *Polymers 16*(14), article 1959. DOI: 10.3390/polym16141959

Jaramillo-Quiceno, N., Vélez R., J. M., Cadena, C., E. M., Restrepo-Osorio, A., and Santa, J. F. (2018). "Improvement of mechanical properties of pineapple leaf fibers by mercerization process," *Fibers and Polymers* 19, 2604-2611. DOI: 10.1007/s12221-018-8522-3

Kanawade, S. M., and Gaikwad, R. W. (2011). "Removal of methylene blue from effluent by using activated carbon and water hyacinth as adsorbent," *International Journal of Chemical Engineering and Applications* 2, 317-319.

Konicki, W., Aleksandrzak, M., and Mijowska, E. (2017). "Equilibrium, kinetic and thermodynamic studies on adsorption of cationic dyes from aqueous solutions using graphene oxide," *Chemical Engineering Research and Design* 123, 35-49. DOI: 10.1016/j.cherd.2017.03.036

Kumar, H., Maurya, K. L., Gehlaut, A. K., Singh, D., Maken, S., Gaur, A., and Suantak, K. (2020). "Adsorptive removal of chromium(VI) from aqueous solution using binary bio-polymeric beads made from bagasse," *Applied Water Science* 10, 1-10. DOI: 10.1007/s13201-019-1101-y

Kuncoro, E. P., T. S., Trisnadi, W. C. P., Handoko, D., Nanda, R. A., and Heri, S. K. (2017). "Characterization of a mixture of algae waste bentonite used as adsorbent for the removal of Pb^{2+} from aqueous solution," *Data in Brief*, DOI: 10.1016/j.dib.2017.12.030i

Liang, F.-B., Song, Y.-L., Huang, C.-P., Zhang, J., and Chen, B.-H. (2013). "Adsorption of hexavalent chromium on a lignin-based resin: Equilibrium, thermodynamics, and kinetics," *Journal of Environmental Chemical Engineering* 1, 1301-1308.

Liang, X., Fan, X., Li, R., Li, S., Shen, S., and Hu, D. (2018). "Efficient removal of Cr(VI) from water by quaternized chitin/branched polyethylenimine biosorbent with hierarchical pore structure," *Bioresour. Technol.* 250, 178-184.

Lai, H. J. (2021). "Adsorption of remazol brilliant violet 5R (RBV-5R) and remazol brilliant blue R (RBBR) from aqueous solution by using agriculture waste," *Tropical Aquatic and Soil Pollution* 1, 11-23.

Misbah, A., Haq, N. B., Munawar, I., Saima, N., and Sana, S. (2016). "Biocomposite efficiency for Cr(VI) adsorption: Kinetic, equilibrium and thermodynamics studies," *Journal of Environmental Chemical Engineering* 5(1), 400-411. DOI: 10.1016/j.jece.2016.12.002

Mthombeni, N. H., Onyango, M. S., and Aoyi, O. (2015). "Adsorption of hexavalent chromium onto magnetic natural zeolite-polymer composite," *Journal of Taiwan Institute of Chemical Engineers* 50, 242-251. DOI: 10.1016/j.jtice.2014.12.037

Neolaka, Y. A. B., Baunsele, S. D., Nitbani, F. O., de Rozari, P., Widyaningrum, B. A., Lawa, Y., Amenaghawon, A. N., Darmokeosoemo, H., and Kusuma, H. S. (2024). "Preparation of cellulose adsorbent based on banana peel waste (*Musa paradisiaca*): Green activation and adsorption of Rhodamine B from the aquatic environment," *Nano-Struct. & Nano-Obj*. 38, 101146. DOI: 10.1016/j.nanoso.2024.101146

Ofudje, E.A., Al-Ahmary, K.M., Alzahrani, E.A., Ud Din, S., and Al-Otaib J.S. (2024a). "Sugarcane Peel Ash as a Sorbent for Methylene Blue," *BioResources* 19(4), 9191-9219.

Ofudje, E. A., Al-Ahmary, K. M., Alshdoukhi, I. F., Alrahili, M. R., Kavil, Y. N., Saad Alelyani, S., Bakheet, A. M., and Al-Sehemi, G. (2024b). "Nano round polycrystalline adsorbent of chicken bones origin for Congo red dye adsorption," *Scientific Reports* 14, article 7809. DOI: 10.1038/s41598-024-57412-4

Ofudje, E. A., Sodiya, E. F., Akinwunmi, F., Ogundiran, A. A., Oladeji, O. B., and Osideko, O. A. (2022). "Eggshell derived calcium oxide nanoparticles for toluidine blue removal," *Desalination and Water Treatment* 247, 294-308. DOI: 10.5004/dwt.2022.28079

Ofudje, E. A., Adeogun, A. I., Idowu, M. A., Kareem, S. O., and Ndukwe, N. A. (2020). "Simultaneous removals of cadmium (II) ions and reactive yellow 4 dye from aqueous solution by bone meal derived apatite: Kinetics, equilibrium and thermodynamic evaluations," *Journal of Analytical Science and Technology* 11, article 7. DOI: 10.1186/s40543-020-0206-0

Ofudje, E. A., Awotula, A. O., Oladipo, G. O., and Williams, O. D. (2014). "Detoxification of chromium (VI) ions in aqueous solution via adsorption by raw and activated carbon prepared from sugarcane waste," *Covenant Journal of Physical and Life Sciences* 2, 110-122.

Ogundiran, A. A., Ololade, O. B., Ogundiran, O. O., and Ofudje, E. A. (2022). "Utilization of unmodified and acid modified snail shells as low-cost adsorbents for the removal of Congo red," *Mountain Top University Journal of Applied Science and Technology* 2, 27-38.

Ozsin, G., Kılıç, M., Apaydın-Varol, E., and Pütün, A. E. (2019). "Chemically activated carbon production from agricultural waste of chickpea and its application for heavy metal adsorption: Equilibrium, kinetic, and thermodynamic studies," *Applied Water Science* 9, 1-14. DOI: 10.1007/s13201-019-0942-8

Parlayici, Ş., and Pehlivan, E. (2019). "Comparative study of Cr(VI) removal by bio-waste adsorbents: Equilibrium, kinetics, and thermodynamic," *Journal of Analytical Science and Technology* 10, article Number 15. DOI: 10.1186/s40543-019-0175-3

Peñas, F. J., Romo, A., and Isasi, J. R. (2022). "Removal of cresols from water by packed beds of cyclodextrin-based hydrogels," *Journal of Polymers and the Environment* 30, 1189-1198. DOI: 10.1007/s10924-021-02259-3

Qian, Q., Machida, M., and Tatsumoto, H. (2008). "Textural and surface chemical characteristics of activated carbons prepared from cattle manure compost," *Waste Mgt.* 28(6), 1064-1071. DOI: 10.1016/j.wasman.2007.03.029

Raseed, A. K., Munawar, I., Aftab, A., Syeda, M. H., Arif, N., Abida, K., Heri, S. K., Jan, N., Nasir, M., Umer, Y., Rab, N., and Muhammad, I. K. (2020). "Kinetics and equilibrium studies of copper, zinc, and nickel ions adsorptive removal on to

Archontophoenix alexandrae: Conditions optimization by RSM," *Desalin. and Water Treat.* 201, 289-300. DOI: 10.5004/dwt.2020.25937

Reddy, K. O., Maheswari, C. U., Dhlamini, M. S., Mothudi, B. M., Kommula, V. P., Zhang, J., Zhang, J., and Rajulu, A. V. (2018). "Extraction and characterization of cellulose single fibers from native African Napier grass," *Carbohydrate Polymer* 188, 85-91. DOI: 10.1016/j.carbpol.2018.01.110

Salahuddin, N., Abdelwahab, M. A., Akelah, A., and Elnagar, M. (2020). "Adsorption of Congo red and crystal violet dyes onto cellulose extracted from Egyptian water hyacinth," *Natural Hazards.* DOI: 10.1007/s11069-020-04358-1

Salman, M., Demir, M., Tang, H. H. D., Cao, L. T. T., Bunrith, S., Chen, T.-W., Darwish, N. M., Almenqedhi, B. M., and Hadibarata, T. (2022). "Removal of cresol red by adsorption using wastepaper," *Industrial and Domestic Waste Management* 2(1), article 63. DOI: 10.53623/idwm.v2i1.63

Sanad, M. N., Farouz, M., ElFaham, M. M., El-Hussein, A., Abd El-sadek, M. S., Althobiti, R. A., and Loanid, A. (2024). "Review: Recent developments in the implementation of activated carbon as heavy metal removal management," *Water Conserv Sci Eng* 9, article 62. DOI: 10.1007/s41101-024-00287-3

Satyam, S., and Sanjukta, P. (2024). "Innovations and challenges in adsorption-based wastewater remediation: A comprehensive review," *Heliyon* 10, article e29573. DOI: 10.1016/j.heliyon.2024.e29573

Shabiimam, M. A., and Anil, K. D. (2012). "Adsorption of o-cresol in landfill leachate using activated carbon," *International Journal of Environmental Science and Development* 3(2), 189-193.

Samaraweera, A. P. G. M. V., Priyantha, N., Gunathilake, W. S. S., Kotabewatta, P. A., and Kulasooriya, T. P. K. (2020). "Biosorption of Cr(III) and Cr(VI) species on NaOH-modified peel of *Artocarpus nobilis* fruit. 1. Investigation of kinetics," *Applied Water Science* 10, 1-11. DOI: 10.1007/s13201-020-01187-2

Shi, X., Qiao, Y., An, X., Tian, Y., and Zhou., H. (2020). "High-capacity adsorption of Cr(VI) by lignin-based composite: Characterization, performance and mechanism," *International Journal of Biological Macromolecules* 159, 839-849. DOI: 10.1016/j.ijbiomac.2020.05.130

Singh, S. R., and Singh, A. P. (2012). "Treatment of water containing chromium (VI) using rice husk carbon as a new low cost adsorbent," *International Journal of Environmental Research* 6, 917-924.

Taleb, Z., Ramdani, A., Berenguer, R., Ramdani, N., Adjir, M., and Talib, S. (2021). "Combined ozonation process and adsorption onto bentonite natural adsorbent for the o-cresol elimination," *International Journal of Environmental Analytical Chemistry* 103(5), 977-994. DOI: 10.1080/03067319.2020.1865335

Tkaczyk, A., Mitrowska, K., and Posyniak, A. (2020). "Synthetic organic dyes as contaminants of the aquatic environment and their implications for ecosystems: A review," *Science of The Total Environment* 717, article ID 137222. DOI: 10.1016/j.scitotenv.2020.137222

Uzosike, A. O., Ofudje, E. A., Adeogun, A. I., Akinyele, J. O., and Idowu, M. A. (2022). "Comparative analysis of bisphenol-A removal efficiency from water: Equilibrium, kinetics,thermodynamics and optimization evaluations," *Journal of the Iranian Chemical Society* 19, 4645-4658. DOI: 10.1007/s13738-022-02628-2

Wahlstrom, N., Edlund, U., Pavia, H., Toth, G., Jaworski, A., Pell, A. J., Choong, F. X., Shirani, H., Nilsson, K. P. R., and Richter-Dahlfors, A. (2020). "Cellulose from the

green macroalgae *Ulva lactuca*: Isolation, characterization, optotracing, and production of cellulose nanofibrils," *Cellulose* 27, 3707-3725. DOI: 10.1007/s10570-020-03029-5

Wu, M., Li, G., Jiang, X., Xiao, Q., Niu, M., Wang, Z., and Wang, Y. (2017). "Non-biological reduction of Cr(vi) by reacting with humic acids composted from cattle manure," *RSC Advances* 7(43), 26903-26911. DOI: 10.1039/c6ra28253a

Yang, X., Li, L., Zhao, W., Wang, M., Yang, W., Tian, Y., Zheng, R., Deng, S., Mu, Y., and Zhu, X. (2023). "Characteristics and functional application of cellulose fibers extracted from cow dung wastes," *Materials* 16(2), article 648. DOI: 10.3390/ma16020648

Yang, F., Lu, Y., Dong, X., Liu, M., Li, Z., Wang, X., Li, L., Zhu, C., Zhang, W., Yu, C., *et al.* (2022). "Interfacial engineering coupling with tailored oxygen vacancies in $Co_2Mn_2O_4$ spinel hollow nanofiber for catalytic phenol removal," *Journal of Hazardous Materials* 424(Part C), article ID 127647. DOI: 10.1016/j.jhazmat.2021.127647

Yogeshwaran, V., and Priya, A. K. (2017). "Removal of hexavalent chromium (Cr^{6+}) using different natural adsorbents A review," *SSRN Electronic Journal* 2017, article ID 3090245. DOI: 10.2139/ssrn.3090245

Zhang, H., Lu, J., Peng, J., Du, G., Peng, H., and Fang, Y. (2018). "One-step preparation of emulsion-templated amino-functionalized porous organosilica monoliths for highly efficient Cr(VI) removal," *Colloids and Surfaces A: Physicochemical and Engineering Aspects* 555, 8-17.

Zhang, Z, Wang, L., and Zhou, X, (2023). "Study on adsorption behaviors of different cresols: First-principles calculation," Journal of Molecular Liquids 390(Part B), article ID 123120. DOI: 10.1016/j.molliq.2023.123120

Zhu, Y., and Kolar, P. (2016). "Investigation of adsorption of *p*-cresol on coconut shell-derived activated carbon," *Journal of Taiwan Institute of Chemical Engineers* 68, 138-146. DOI: 10.1016/j.jtice.2016.07.044

Article submitted: October 21, 2024; Peer review completed: January 21, 2025; Revised version received: February 5, 2025; Accepted: February 27, 2025; Published: March 11, 2025.
DOI: 10.15376/biores.20.2.3252-3285